

Determining lake surface water temperatures (LSWTs) worldwide using a tuned 1-dimensional lake model (*FLake*, v1)

List of Authors	Afiliations
Dr A. Layden	4 Rose Hill, Sligo, Ireland Email: aislinglayden99@gmail.com Phone: +353 (0) 86 345 3404
Dr S. N. MacCallum	The university of Edinburgh, School of Geosciences, Grant Institute, The King's Buildings, West Mains Road, Edinburgh EH9 3FE Email: stuart.maccallum@gmail.com
Dr C. J. Merchant	Dept. of Meteorology, University of Reading Harry Pitt Building, 3 Earley Gate, PO Box 238, Whiteknights, Reading, RG6 6AL Email: c.j.merchant@reading.ac.uk

1 Abstract

2

3

4 A tuning method for *FLake*, a 1-dimensional freshwater lake model, is applied for the
5 individual tuning of 244 globally distributed large lakes using observed lake surface water
6 temperatures (LSWTs) derived from Along-Track Scanning Radiometers (ATSRs). The
7 model, which was tuned using only 3 lake properties (lake depth, snow and ice albedo and
8 light extinction coefficient), substantially improves the measured mean differences in
9 various features of the LSWT annual cycle, including the LSWTs of saline and high
10 altitude lakes, when compared to the observed LSWTs. Lakes whose lake-mean LSWT
11 persists below 1 °C for part of the annual cycle are considered to be 'seasonally ice-
12 covered'. For trial seasonally ice-covered lakes (21 lakes), the daily mean and standard
13 deviation (2σ) of absolute differences between the modelled and observed LSWTs, are
14 reduced from 3.07 ± 2.25 °C to 0.84 ± 0.51 °C by tuning the model. For all other trial lakes
15 (14 non-ice covered lakes), the improvement is from 3.55 ± 3.20 °C to 0.96 ± 0.63 °C. The
16 post tuning results for the 35 trial lakes (21 seasonally ice-covered lakes and 14 non-ice
17 covered lakes) are highly representative of the post-tuning results of the 244 lakes.

18

19 For the 21 seasonally ice-covered lakes, the modelled response of the summer-LSWTs to
20 changes in snow and ice albedo is found to be statistically related to lake depth and
21 latitude, which together explain 0.50 ($R^2_{\text{adj}}, p = 0.001$) of the inter-lake variance in summer
22 LSWTs. Lake depth alone explains 0.35 ($p = 0.003$) of the variance.

23

24 Lake characteristic information (snow and ice albedo and light extinction coefficient) is not
25 available for many lakes. The approach taken to tune the model, bypasses the need to
26 acquire detailed lake characteristic values. Furthermore, the tuned values for lake depth,
27 snow and ice albedo and light extinction coefficient for the 244 lakes provide some
28 guidance on improving *FLake* LSWT modelling.

29

30

31

1 Introduction

2
3 The response of LSWTs to climate is highly variable and is influenced by lake physical
4 characteristics (Brown and Duguay, 2010). Some large lakes have been shown to alter the
5 local climate. The extent of ice cover on lakes is considered to be a sensitive indicator of
6 and also a factor in global change (Launiainen and Cheng, 1998). Changes in the length of
7 the ice cover period affect local climatic feedbacks; for example, a shorter ice cover period
8 allows a longer time for surface heat exchange with the atmosphere (Ashton, 1986). This is
9 of particular importance in areas where there is a high concentration of lakes, such as
10 Canada (Pour et al., 2012). The fluxes of heat and moisture from the Great Lakes and the
11 large Canadian lakes of Great Bear and Great Slave can impact the mesoscale weather
12 processes causing lake-effect storms, altering the local climate (Sousounis and Fritsch,
13 1994; Long et al., 2007). Shallow lakes, particularly those with a large surface area, such
14 as Lake Balaton, are more sensitive to atmospheric events (Voros et al., 2010).

15
16 Reliable modelling of LSWTs can enrich our understanding of the highly variable dynamic
17 nature of lakes. In this paper, a freshwater lake model, *FLake* (available at
18 <http://www.flake.igb-berlin.de/sourcecodes.shtml>), is tuned with ATSR Reprocessing for
19 Climate: Lake Surface Water Temperature and Ice Cover (ARC-Lake) observations
20 (MacCallum and Merchant, 2012) of 244 globally distributed lakes. *FLake* is a 1-
21 dimensional thermodynamic lake model, capable of predicting the vertical temperature
22 structure and mixing conditions of a lake (Mironov et al, 2010). The tuned model is
23 expected to improve the LSWT representation of these lakes in *FLake*.

24
25 There have been some studies carried out that compare modelled LSWTs from *FLake* with
26 LSWT observations on European lakes (Voros et al., 2010; Bernhardt et al., 2012; Pour et
27 al., 2012). The findings from two of these three studies showed consistent differences
28 between the modelled and observed LSWTs (overestimation of the open water LSWTs and
29 underestimation of the ice cover period). Despite these differences, *FLake* is considered to
30 be a reliable model for simulating LSWTs and lake ice phenology (Bernhardt et al., 2012).
31 The overestimation of the open water LSWTs and underestimation of the ice cover period

1 are consistent with preliminary trial work findings from this study, which included North
2 American and European lakes.

3
4 It is the intention of this study to achieve a daily mean absolute difference (MAD) of ≤ 1
5 $^{\circ}\text{C}$, between the tuned and observed LSWTs, across all lakes. For each lake, the daily MAD
6 quantifies the mean absolute difference in modelled and observed daily LSWT value,
7 averaged over the total number of days. The dispersion of the daily MADs are reported to
8 2 standard deviations ($\pm 2\sigma$) for each lake. When reported across a number of lakes, the
9 daily MAD for each lake is averaged, with the dispersion of the MADs across individual
10 lakes reported to 2 standard deviations ($\pm 2\sigma$).

11
12 A daily MAD of ≤ 1 $^{\circ}\text{C}$ across all lakes, is possibly accurate enough for a global scale
13 study. A lower daily MAD target may not be achievable as this study comprises of lakes
14 with a wide range of geographical and physical characteristics. The effect of the tuning on
15 the sub-surface temperature profile and on the depth of the mixed layer is not considered in
16 this study. Many lake-specific properties can be considered in *FLake*. Preliminary model
17 trial work was carried out on 7 seasonally ice-covered lakes (deep and shallow) which had
18 available lake characteristic data in the ILEC world lake database (<http://wldb.ilec.or.jp/>)
19 or LakeNet (www.worldlakes.org). Through this preliminary work, the lake-specific
20 properties which exerted the strongest effect on the modelled LSWTs were selected. These
21 properties are lake depth (d), snow and ice albedo (α) and light extinction coefficient (κ).
22 In the next part of the preliminary work, it was determined that the modelled LSWTs could
23 be tuned to compare well with the observed LSWTs, by adjusting the values for these three
24 properties: d , α and κ , herein referred to LSWT-regulating properties. On the basis of the
25 preliminary findings, the trial work was performed on 35 lakes, prior to attempting to tune
26 all 246 lakes.

27
28 An example of the preliminary trial work is shown in Fig. 1a, Lake Athabasca, Canada
29 (mean depth of 26 m). In this figure, a greater modelled α (higher reflectivity) results in a
30 later ice-off date than the default model snow and ice albedo and is closely comparable to
31 the observed ice-off date. In Fig. 1b, it is demonstrated that by using a shallower d than the
32 mean depth of the lake, the ice-on day occurs earlier and corresponds more closely to the

1 observed ice-on day. Lake depth is essentially being used as a means to adjust the heat
2 capacity of the lake, exerting control over the lake cooling and therefore the ice-on date.
3 The modelled LSWT is further improved by lowering the κ value (greater transparency).
4 The greater transmission of surface heat to the lower layer results in a lower (and more
5 representative) maximum LSWT, Fig. 1b. The LSWTs modelled using the greater α , lower
6 d and lower κ compare closely with the observed LSWTs, Fig. 1c.

7

8 In this study, the modelled mean differences for several features in the LSWT annual cycle
9 are measured, quantifying the level of agreement with the observed ARC-Lake LSWTs,
10 are the basis for selecting the tuned (optimal) LSWT-regulating properties (d , α and κ) for
11 each lake. Lakes are divided into 2 distinct categories. Lakes with a lake-mean LSWT
12 climatology (determined using twice-a-month ARC-Lake full year LSWT observations,
13 1992/1996–2011) remaining below 1 °C for part of the seasonal cycle are categorised as
14 seasonally ice-covered lakes (160 lakes). All other lakes are categorised to as non-ice
15 covered lakes (86 lakes). Although some of the seasonally ice-covered lakes may not be
16 completely ice-covered during the cold season and some of the non-ice covered lakes may
17 have short periods of partial ice cover, the 1 °C lake-mean LSWT offers a good means of
18 evaluating lakes that are typically and non-typically ice-covered during the coldest part of
19 the LSWT cycle. To best capture the critical features of both seasonally ice-covered and
20 non-ice covered lakes, the mean difference in the features between the observed and
21 modelled LSWTs differ with lake category. The tuning approach applied to these two lake
22 categories is summarised in Fig. 2, and described in detail within Sect. 2.3.

23

24 Using the observed LSWTs (ARC-Lake), the objective of this study is to assess if *FLake*
25 can be tuned to produce realistic LSWTs for large lakes globally, using relatively few lake
26 properties. It is expected that for each lake, the tuning of lake properties will compensate to
27 a greater or lesser degree for some of the lake to lake variability in geographical and
28 physical characteristics. The motivation for this study was to develop a greater
29 understanding of lake dynamics globally, offering the potential to help develop
30 parameterization schemes for lakes in numerical weather prediction models. It is expected
31 that the findings in this study will be of interest to climate modellers, limnologists and
32 current and perspective users of *FLake*.

1
2
3
4
5
6
7
8
9
10
11
12
13
14
15
16
17
18
19
20
21
22
23
24
25
26
27
28
29
30
31

2 Methods

2.1 Data: ARC-Lake observed LSWTs

LSWT observations from ARC-Lake are used to tune the model. These cover 246 globally distributed large lakes, principally those with surface area $> 500\text{km}^2$ (Herdendorf, 1982; Lehner and Döll, 2004) but also including 28 globally distributed smaller lakes, the smallest of which is 100 km^2 (Lake Vesijarvi, Finland). The LSWTs are generated from three Along-Track Scanning Radiometers (ATSRs), from August 1991– December 2011 (MacCallum and Merchant, 2012).

The ARC-Lake observations have been shown to compare well with in situ LSWT data, demonstrating their suitability for use in this study. Validation of the observations was performed through a match-up data set of in situ temperature data consisting of 52 observation locations covering 18 of the lakes (MacCallum and Merchant, 2012). The timing of ice-on and ice-off events is observed to be consistent with in situ measurements. This is demonstrated through analysis of the average (over the period of ATSR observations) days of the year on which the lake-mean LSWT drops below $1\text{ }^\circ\text{C}$ and rises above $1\text{ }^\circ\text{C}$. Layden et al. (2015) define these as the $1\text{ }^\circ\text{C}$ cooling and $1\text{ }^\circ\text{C}$ warming days respectively, and observe good consistency with in situ measurements of ice-on and ice-off days for 21 Eurasian and North American lakes. Layden et al. (2015) also demonstrate the integrity of the ARC-Lake LSWTs on a global scale, through the strong relationship the observed LSWTs have with meteorological data (air temperature and solar radiation) and geographical features (latitude and altitude).

An average of the day and night lake-mean LSWT observations from 08 August 1991 to the end of 2010 is used to tune the model. The final year of observations (2011) is retained to carry out an independent evaluation on the tuned model. For 119 lakes, there are continuous LSWT observations for 20 years (all three ATSR instruments, from August 1991 to December 2011), 113 lakes have 16 years of continuous LSWT observations (2

1 ATSR instruments), and 14 lakes have 8–9 years of LSWT observations (1 ATSR
2 instrument). The location of the 246 lakes (55° S to 69° N), classified by surface area,
3 using polygon area in Global Lakes and Wetlands Database, GLWD (Lehner and Döll,
4 2004), is shown in Fig. 3.

5 6 **2.2 Model; *FLake* lake model**

7
8 *FLake* is a two-layer parametric representation of the evolving temperature profile of a
9 lake and is based on the net energy budgets (Mironov, 2008). The depth and temperature of
10 the homogeneous ‘upper mixed layer’ and the temperature of the ‘lake-bottom’
11 (representative of the hypolimnion temperature) as illustrated in Fig. 4, are modelled in
12 *FLake*. The thermal structure of the intermediate stratified layer (thermocline, Fig. 4), is
13 parameterised in *FLake* through a self-similarity representation of the temperature profile,
14 $v(\zeta)$, using time (T) and depth (z) as illustrated in Fig. 5.

15
16 *FLake* utilises the minimum set of input data required for 1-dimensional thermal and ice
17 models: meteorological forcing data (shortwave and long wave radiation, wind speed, air
18 vapour pressure and air temperature), an estimation of turbidity and basic bathymetric data
19 (Lerman et al., 1995). Although models based on the concept of self-similarity are
20 considered to be only fairly accurate (Dutra et al., 2010), we show that modelled mean
21 differences between the model and observed LSWTs are greatly lowered by tuning the
22 model.

23 24 **2.2.1 Lake-specific model properties**

25
26 As outlined in the introduction, optimisation of LSWT-regulating properties (lake depth
27 (d), snow and ice albedo (α) and light extinction coefficient (κ)), can greatly improve the
28 LSWTs simulated in *FLake*. Other lake-specific properties adjusted for this study are:
29 c_relax_C , $fetch$, latitude and the starting conditions.

30

1 *c_relax_C*: a dimensionless constant used in the relaxation equation for the shape factor
2 with respect to the temperature profile in the thermocline.
3 The default value of 0.003 was found to be too low to adequately readjust the temperature
4 profile of deep lakes (G. Kirillin, personal communication, 2010), weakening the predicted
5 stratification and affecting the LSWT. For lakes with mean depths < 5 m, the *c_relax_C*
6 value is set to 10^{-2} , and decreases with increasing depth, to a value of 10^{-5} for mean depths
7 > 50 m, as recommended by G. Kirillin (personal communication, 2010).

8
9 *Fetch*: wind fetch is calculated as the square root of the product of lake length (km) and
10 breadth (km) for the 205 (of 246) lakes with available dimensions. A line-fit on the
11 calculated fetch (km) versus polygon area from the GLWD (Lehner, and Döll, 2004) of
12 these 205 lakes, showed a strong relationship between fetch and area, Eq. (1), $R^2_{adj} = 0.84$,
13 $p = 0.001$. Equation (1), used to determine the fetch of the remaining 41 lakes with no
14 available dimensions, is valid for lakes > 100km². Although the shape of a lake and it's
15 orientation in relation to wind direction are likely to affect wind fetch, this approach is
16 expected to provide reasonable estimates of fetch.

17
18
$$\text{fetch} = 39.9 \text{ km} + (0.00781 \text{ km}^{-1}) \times \text{area in km}^2 \quad (1)$$

19
20 *latitude*: the latitude of the lake centre reference co-ordinates (Herdendorf, 1982; Lehner
21 and Döll, 2004).

22
23 *Starting conditions*: provide the initial lake-specific upper mixed layer temperature and
24 depth, bottom temperature, ice thickness and air–ice interface temperature, were shown to
25 shorten the model spin-up time (to an average of < 3 days). A good estimation of the
26 starting conditions was obtained from the *FLake* model based on the hydrological year
27 2005/06 (Kirillin et al., 2011).

2.2.2 Fixed model parameters

The icewater_flux, inflow from the catchment and heat flux from sediments remain fixed throughout the investigative and tuning process, across all lakes. For icewater_flux, (heat flow from water to ice) G. Kirillin (personal communication, 2010) suggests values of ~ 3–5Wm⁻². In this study a value of 5Wm⁻² is applied to all lakes. Inflow from the catchment and heat flux from sediments are not considered.

2.2.3 Model forcing data

FLake is forced with ECMWF Interim Re-analysis (ERA) data (Dee et al., 2011; ECMWF, 2009), at the grid points (0.7° x 0.7° resolution) closest to the lake centre, shown in the Supplement. The mean daily values of shortwave solar downward radiation (SSRD), air temperature and vapour pressure at 2m, wind speed at 10m, and total cloud cover (TCC), shown in Table 1, are used to force the model.

2.3 Tuning method

A range of factors/values for d , α and κ is determined through the model trials (carried out on 21 seasonally ice-covered lakes and 14 non-ice covered lakes, Fig. 6). These lakes broadly represent the range of lake characteristics – lake depth, snow and ice albedo and light extinction coefficient – and have available Secchi disk depth data.

2.3.1 Light extinction coefficients for trial lakes

The light extinction coefficient values for the untuned model trial are derived from Secchi disk depth data, κ_{sd} (m⁻¹), obtained from the ILEC database (ILEC, 1999). Five methods of relating κ values to Secchi disk depths (Poole and Atkins, 1929; Holmes, 1970; Bukata et al., 1988; Monson, 1992; Armengol et al., 2003) are compared in Fig. 7. These methods cover a range of different water conditions, from coastal turbid waters (Holmes, 1970) and

1 eutrophic water (tested 1 km from a dam in the Sau reservoir, Spain) (Armengol et al.,
2 2003) to a range of North American lakes of different trophic levels (Monson, 1992).

3
4 For Secchi disk depths > 10 m, all methods show a reasonably good comparison between
5 Secchi disk depths and κ , Fig. 7. From Secchi disk depths of 10 to 1 m, the range of results
6 between methods become increasingly large. Bukata et al. (1998) showed that the formula
7 Eq. (2), based on in situ optical measurements from many stations, adequately described
8 Lake Huron, Lake Superior and Lake Ontario, for Secchi disk depths from 2 to 10 m;

9
10
$$\kappa_{sd} = (0.757/ S) + 0.07\text{m}^{-1} \quad (2)$$

11
12 where S = Secchi disk depth (m).

13
14 Eq. (2), applied in this study for lakes with Secchi disk depths of 2-10 m, produces the
15 lowest (most transparent) κ values, potentially more representative of open water
16 conditions of large lakes. For lakes outside this Secchi disk depth range (less than 2 m and
17 greater than 10 m), the Poole and Atkins (1929) formula, Eq. (3), is applied, providing
18 sufficiently accurate estimations of light extinction coefficients in waters with all degrees
19 of turbidity (Sherwood, 1974).

20
21
$$\kappa_{sd} = 1.7/ S \quad (3)$$

22
23 **2.3.2 Light extinction coefficients for tuning of all lakes**

24
25 As many lakes do not have available Secchi disk depth data, an alternative approach is
26 used to provide light extinction coefficients in the tuned model trials and for the tuning of
27 all lakes. A range of 10 optical water types which essentially describe the attenuation
28 process of ocean water and its changes with turbidity (Jerlov, 1976) is applied. These
29 consist of 5 optical water types for open ocean, type I, IA, IB, II and III; type I being the
30 most transparent and type III being least transparent and 5 coastal ocean types (1, 3, 5, 7
31 and 9) (Jerlov, 1976). The spectrum for these 10 ocean water types are divided (in fractions

1 of 0.18, 0.54, 0.28) into bands represented by three wavelengths: 375, 475 and 700nm,
2 respectively. The 10 ocean water types are renamed herein as κ_{d1} to κ_{d10} , the values for
3 which are shown in Table 2.

4 5 **2.3.3 Tuning of lake depth**

6
7 Lake depth information was obtained from Herdendorf (1982), the ILEC World Lake
8 Database (<http://wldb.ilec.or.jp/>), LakeNet (<http://www.worldlakes.org/>) and (Kourzeneva
9 et al., 2012). The mean depth (Z_{d1}) is the recommended depth value for *FLake*. Where only
10 maximum depth is available (9 lakes), the mean depth is calculated using the average
11 maximum-to-mean depth ratio of lakes with known maximum and mean depths. This ratio
12 is 3.5 for seasonally ice-covered lakes and 3.0 for non-ice covered lakes. In the tuning
13 process, depth factors (outlined in Table 2) are applied to the lake-mean depth. The tuned
14 depth is referred to as the ‘effective depth’. For lakes with no depth information, the
15 effective depth factors are applied to a depth of 5 m. If the resulting effective depth is too
16 shallow, characterised by early LSWT cooling and/or a high summertime LSWT; July,
17 August and September (JAS) LSWT, tuning is repeated using a deeper input depth.

18
19 For modelling very deep lakes, a “false depth” is recommended (G. Kirillin, personal
20 communication, 2010). For the 6 lakes with mean depths in excess of 240 m (ranging from
21 240 m for Lake Kivu to 680 m for Lake Baikal), false depths of 100 m – 200 m are used in
22 the tuning study.

23 24 **2.3.4 Tuning of snow and ice albedo**

25
26 *FLake* uses two categories of albedo for snow (dry snow and melting snow) and for ice
27 (white ice and blue ice). As the snow cover module is not operational in this version of
28 *FLake*, the snow and ice albedo are set to the same default value in the albedo module;
29 0.60 for dry snow and white ice and 0.10 for melting snow and blue ice. An empirical
30 formulation is applied in *FLake*, where the albedo of a frozen lake surface (α_{lake}) depends
31 on the ice surface temperature (Eq. 4) (Rooney and Jones, 2010), accounting somewhat for

1 seasonal changes in albedo (Mironov and Ritter, 2004). By application of this equation, the
2 blue ice (by means of it's albedo) has greater influence on the rate of ice melting, in the
3 warming season.

$$4 \quad \alpha_{lake} = \alpha_w + (\alpha_b - \alpha_w) \exp[-C\alpha (T_0 - T_p)/T_0] \quad (4)$$

5 where α_w = white ice albedo (0.60), α_b = blue ice albedo (0.10), $C\alpha$ = Ice albedo empirical
6 coefficient (95.6), T_0 = freezing temperature (K) and T_p = the surface temperature (K)
7 from the previous time step. The extinction coefficient values (m^{-1}) used for modelling
8 solar radiation penetration through white ice and blue ice are 17.1 and 8.4, respectively and
9 correspond to the top 0.1 m of the ice layer for clear sky conditions (Launiainen and
10 Cheng, 1998).

11 The default snow and ice albedo values are referred to as αI in this study. During the
12 preliminary trials, a higher albedo (than αI) was shown to delay ice-off, substantially
13 improving the timing of early ice-off, compared to observed LSWTs (demonstrated in Fig.
14 1a). A higher snow and ice albedo causes more of the incoming radiation to be reflected,
15 resulting in a later ice-off. On this basis, we apply 3 additional higher albedo values ($\alpha 2$:
16 $\alpha 4$), shown in Table 2, for tuning seasonally ice-covered lakes. Albedo when discussed
17 throughout this study refers to the albedo of snow and ice. The albedo of water (in liquid
18 phase) is maintained at the default value of 0.07 throughout this study.

19

20 **2.3.5 Wind speed scaling**

21

22 Scaling of wind speeds is considered during the trials, as most long-term records of wind
23 speed are measured over land (U_{land}) and are considered to underestimate the wind speed
24 over water (U_{water}). For adjusting surface wind speeds (measured in m/s) over land to wind
25 speeds over sea surfaces, Hsu (1988) recommends the scaling shown in Eq. (5). For bodies
26 of water with fetch > 16 km, a scaling of 1.2 applied to over-land wind speeds (measured
27 at a height of 10 m) provide reasonable estimates of wind speeds over sea surfaces (Resio
28 et al., 2008). To find a suitable wind speed scaling, the trial work is carried out using the
29 unscaled wind speed ($u1$), wind speed factored by 1.2 ($u2$), and wind speed suggested by

1 Hsu (1988), u_3 (Eq. 5). During the trial work, the most appropriate wind speed scalings are
2 determined.

3
4
$$U_{\text{water}} = 1.62 \text{ m/s} + 1.17U_{\text{land}} \quad (5)$$

5
6 Where U_{water} = wind speed over water (m/s), U_{land} = surface wind speed over land (m/s)

7
8 **2.3.6 Summary of the tuning of the LSWT-regulating properties**

9
10 Table 2 contains a summary of the factors/values for d , α and κ applied in this tuning
11 study. The model is tuned using the optimal combination of LSWT-regulating properties;
12 80 possible combinations for seasonally ice-covered lakes and 60 possible combinations
13 for non-ice covered lakes.

14
15 **2.4 Tuning metrics**

16
17 The tuning metrics are the mean differences (between the modelled and the observed
18 LSWTs), used to quantify the effect that the LSWT-regulating properties have on the
19 modelled LSWTs. The metrics (normalised and equally weighted) determine the optimal
20 LSWT model selected for each lake.

21
22 **2.4.1 Tuning metrics for seasonally ice-covered lakes**

23
24 The metrics and the effect of the LSWT-regulating properties on them, for seasonally ice-
25 covered lakes is summarised in Table 3. The effect of light extinction coefficient on the
26 JAS LSWTs is demonstrated in Fig. 8, showing that the tuned light extinction coefficient
27 (κ_d) value, κ_{d6} in place of a lower (more transparent) κ_d value (κ_{d2}), described in Table 2,
28 substantially improves the JAS LSWT. In this figure, the greater effect of light extinction
29 coefficient on the maximum LSWT than on the minimum LSWT is also demonstrated. The
30 influence of the effective depth over the 1 °C cooling day (the day the lake-mean LSWT

1 drops below 1 °C; an indicator of ice-on) is demonstrated in Fig. 9. The 1 °C warming day
 2 (the day the lake-mean LSWT rises to above 1 °C; an indicator of ice-off), is strongly
 3 influenced by snow and ice albedo, as demonstrated in Fig.1a.

4 **2.4.2 Tuning metrics for non-ice covered lakes**

6
 7 For these lakes, the daily MAD and the difference between the observations and model for
 8 the months where the minimum and maximum observed LSWTs occur ($month_{min}$ and $month_{max}$)
 9 are applied as metrics. Although there no definitive stages in the LSWT cycle for non-ice
 10 covered lakes, the $month_{min}$ and $month_{max}$ exert some control over temporally reconciling the
 11 modelled monthly extremes with the observed monthly extremes.

13 **2.4.3 Additional metrics for seasonally ice-covered lakes and non-ice covered lakes**

14
 15 For each lake, the fraction of the observed mean LSWT variance over the number of years
 16 with observations (K^2), accounted for in the tuned model is used to help independently
 17 evaluate the tuned LSWTs. For non-ice covered lakes, the variance is determined using
 18 var_{min} (and var_{max}): the variance in the mean LSWT for the month in which the minimum
 19 (and maximum) LSWT is observed. For seasonally ice-covered lakes, the variance is
 20 determined using var_{jas} : the variance in the observed mean JAS LSWT. The fraction of
 21 these observed LSWT variances accounted for in the tuned model are quantified; $inter_{min}$,
 22 $inter_{max}$ and $inter_{jas}$ (R^2_{adj}), respectively. The calculations to quantify var_{jas} and $inter_{jas}$ are
 23 shown in Eqs. (6) to (8).

24
 25 var_{jas} : (K^2) observed JAS LSWT variance over the length of the tuning period;

$$26 \quad var_{jas} = \sum (x_i^{obs_jas} - \bar{x})^2 / (N - 1) \quad (6) \quad (\text{Walker and Shostak, 2010})$$

27 where x^{obs_jas} = observed mean JAS LSWT for each individual year

28 \bar{x} = mean across all years

29 N = number of years with JAS LSWTs

1
2
3
4
5
6
7
8
9
10
11
12
13
14
15
16
17
18
19
20
21
22
23
24
25
26
27
28
29
30

$inter_{jas}$: the fraction (R^2_{adj}) of the observed JAS LSWT inter-annual variance (var_{jas}) accounted for in the tuned model;

$$inter_{jas} = 1 - ((1 - r^2) (N - 1) / (N - P - 1)) \quad (7) \quad (\text{Lane et al, 2016})$$

P = total number of regressors

$$r^2 = \frac{N \sum (x_i^{obs_jas} - \bar{x}_i^{mod_jas}) \sum (x_i^{mod_jas} - \bar{x}_i^{obs_jas})}{(N \sum (x_i^{mod_jas} - \bar{x}_i^{mod_jas})^2) (N \sum (x_i^{obs_jas} - \bar{x}_i^{obs_jas})^2)} \quad (8) \quad (\text{Walker and Shostak, 2010})$$

where mod_jas = modelled JAS LSWT.

The same equations, Eqs. (6) to (8), are applied to determine $Inter_{max}$, var_{max} , $Inter_{min}$ and var_{min} , substituting “JAS” with “max” and “min”,

where obs_min (and mod_min) = mean observed LSWT (and modelled LSWT) in the month where the minimum LSWT occurs, and

where obs_max (and mod_max) = mean observed LSWT (and modelled LSWT) in the month where the maximum LSWT occurs

3 Trial results for wind speed scaling

For both seasonally ice-covered lakes and non-ice covered lakes, wind speeds, $u1$, $u2$ and $u3$ were modelled with untuned LSWT properties: mean lake depth (Z_{dl}), default snow and ice albedo (αI) and light extinction coefficient derived from Secchi disk depth data (κ_{sd}).

The trials show that wind speed has a consistent effect on the modelled LSWT of seasonally ice-covered lakes. The higher wind speed scaling ($u3$) causes earlier cooling and later warming (reducing the 1 °C cooling day and 1 °C warming day mean differences), lengthening the ice cover period and lowering the JAS LSWT, as demonstrated for Lake Simcoe, Canada in Fig. 10. It is expected that the tuning of d , α and

1 κ , with an applied wind speed of $u3$, will produce modelled LSWTs substantially closer to
2 the observed LSWTs than those shown in Fig. 10, where tuning of d , α and κ is not
3 applied. The more rapid mixing and heat exchange between the surface and atmosphere, as
4 a result of the higher wind speed, causes an earlier modelled 1 °C cooling day. As wind
5 promotes ice growth in the model, higher wind speeds also contribute to the later modelled
6 1 °C warming day. Wind speed scaling, $u3$ in place of $u1$, for the trial seasonally ice-
7 covered lakes, reduces the mean difference in the length of the average cold phase (when
8 compared to the observed cold phase) by ~ 50% (from 39 to 21 days) and reduces the JAS
9 LSWT mean difference by ~ 50%, from 3.71 to 1.87 °C, Table 4. For non-ice covered trial
10 lakes, 5 of the 7 lakes at latitudes > 35° N/S show best results with $u3$, as demonstrated for
11 Lake Biwa, located at 35.6° N, Fig. 11a. Five (5) of the 7 lakes located < 35° N/S show
12 best results with $u1$, as demonstrated for Lake Turkana, located at 3.5° N, Fig. 11b.

13

14 For the remainder of the tuning trials (tuned using the range of d , α and κ factors/values
15 outlined in Table 2), wind speed scaling $u3$ was applied to all seasonally ice-covered and to
16 non-ice covered lakes > 35 °N/S and no scaling ($u1$) to non-ice covered lakes < 35 °N/S.
17 As the target daily MAD of < 1.0 °C is met for both lake categories (shown in the second
18 results column in Table 5), the tuning approach described here is applied to all lakes.

19

20 **4 Results**

21

22 **4.1 Summary of results**

23

24 The daily MAD and spread of differences (2σ) between the modelled and observed
25 LSWTs, across the seasonally ice-covered lakes and non-ice covered lakes, is reduced
26 from 3.07 ± 2.25 and 3.55 ± 3.20 °C for the untuned model to 0.84 ± 0.51 and 0.96 ± 0.63
27 °C for the tuned model, Table 5. The tuned values for the LSWT-regulating properties for
28 all lakes and the tuning metrics are shown in the Supplement.

29

1 These results demonstrate that the tuning process with the applied wind speed scalings can
2 provide significant improvements on the untuned model: run using the lake mean depth,
3 light extinction coefficients derived from Secchi disk depth (as shown in Sect. 2.3.1) and
4 the model default albedo (seasonally ice-covered lakes only).

5
6 The applied tuning method yielded a daily MAD of 0.74 ± 0.48 °C, across 135 of the 160
7 seasonally ice-covered lakes, Table 6. The remaining 25 seasonally ice-covered lakes
8 yielded comparatively poor results; the 1 °C cooling day was 14 days too early and/or the
9 JAS LSWT was ≥ 2 °C higher than observed LSWTs. Re-tuned using greater effective
10 depth factors and higher κ_d values, as outlined in the next sub-section (Sect. 4.1.1), yielded
11 a daily MAD of 1.11 ± 0.56 °C, across the 25 lakes. Across the 160 lakes, a daily MAD of
12 below 1 °C was achieved (0.80 ± 0.56 °C, Table 5). A daily MAD of below 1 °C is again
13 achieved (0.96 ± 0.66 °C) when 84 of the 86 non-ice covered lakes are considered (Table
14 5). The remaining 2 lakes yielded highly unsatisfactory results.

16 **4.1.1 Seasonally ice-covered lakes**

17
18 The 25 lakes that were re-tuned are shallow (average mean depth < 5 m) and small (18 of
19 the 25 lakes are < 800 km²), relative to the depth and area of the larger seasonally ice-
20 covered lakes. Twenty (20) of the 25 lakes are located in Eastern Europe or Asia, at
21 relatively low altitudes; 22 of the 25 lakes are < 752 m a.s.l.. On initial tuning, these 25
22 lakes were tuned to the highest depth factor, Z_{d4} (1.5 times the mean depth) and/or the
23 highest light extinction coefficient, κ_{d5} (lowest transparency). Although the transparencies
24 for these 25 lakes are largely unknown, shallow lakes generally have poorer light
25 transparencies than deeper lakes due to upwelling of bottom sediment. The shallow depth
26 of the modelled lake (lower heat capacity) and the poor transparency of water (more heat
27 retained in surface) were evident in the metric results; early 1 °C cooling day and/or high
28 JAS LSWT values. A modified tuning set-up, to allow for a greater modelled depth to
29 increase the heat capacity - postponing the 1 °C cooling day - and lower transparency
30 values (higher κ_d), causing less heat to be retained in the surface and lowering the JAS
31 LSWT, is applied to these 25 lakes.

1
2
3
4
5
6
7
8
9
10
11
12
13
14
15
16
17
18
19
20
21
22
23
24
25
26
27
28
29
30

The tuning set-up modified to include 3 greater depth factors of 2.5, 2 and 4 times the mean depth (Z_{d6} , Z_{d7} and Z_{d8}) and 2 higher light extinction coefficient values, κ_{d6} and κ_{d7} (Table 2), substantially improves the 1 °C cooling day and the JAS LSWT for these 25 lakes. A summary of the results are shown in Table 6 column 2. The tuning metric results for all 160 lakes (using the modified tuning set-up for the 25 shallow lakes) are illustrated in Fig. 12.

4.1.2 Non-ice covered lakes

The tuning metric results for each of the 84 lakes are illustrated in Fig.13 and a summary of these results are shown in Table 5.

The poor tuning results, observed for 2 of the 86 lakes (Lake Viedma and the Dead Sea) are most likely due to differences between the altitude of the ERA T2 air temperature (geopotential height) and the lake altitude. Lake Viedma, an Argentinian freshwater lake of unknown depth, yielded a daily MAD of 3.1 °C. The Dead Sea, a deep and highly saline lake (340 g L^{-1}) located in Asia at 404 m below sea level, yielded a daily MAD of 4.1 °C.

For the Dead Sea, a temperature difference (in the month of maximum temperature) between the observed LSWT (33 °C) and ERA T2 air temperature (25 °C), results in a negative modelled mean difference of 6.3 °C in LSWT for this month. Given the standard air temperature lapse rate (6.5 °C km^{-1}), altitude can explain the substantially lower air temperatures. The altitude of Dead Sea (-404 m a.s.l.), is lower by $\sim 850 \text{ m a.s.l.}$ than the altitude of the meteorological data at the lake centre co-ordinates, 445 m a.s.l. (determined by interpolating surrounding cells using the orography data accompanying the ECMWF meteorological data).

For Lake Viedma, while the observed LSWTs range from 5 to 10 °C, the minimum ERA T2 air temperature remains well below 0 °C for many months of year, regularly reaching

1 -8 °C, resulting in a negative modelled mean difference of 4.8 °C for the month of
2 minimum LSWT. This difference can be, at least, partially explained by the difference in
3 altitude (> 500 m a.s.l.) between the altitude of Lake Viedma (297 m a.s.l.) and the altitude
4 of meteorological data (825 m a.s.l.) at the lake centre co-ordinates.

6 **4.2 Tuning of saline and high altitude lakes**

8 The tuned metrics shown in Table 7 (seasonally ice-covered lakes) and in Table 8 (non-ice
9 covered lakes) indicate that *FLake* is successful for tuning both saline and high altitude
10 lakes, as well as freshwater and low altitude lakes.

12 Although the density of freshwater in *FLake* is determined at sea level (normal
13 atmospheric pressure) (Mironov, 2008) and the altitude of lakes are not directly considered
14 in *FLake*, lake altitude (ranging from -12 to 5000 m a.s.l., over the 246 lakes) is considered
15 indirectly through the altitude of the meteorological forcing data (ERA) at the lake centre
16 co-ordinates.

18 The majority of the high altitude lakes are also saline; 7 of the 10 non-ice covered lakes
19 and 12 of the 14 seasonally ice-covered lakes. The good comparability of the observed and
20 modelled LSWTs for two high altitude lakes (> 1500 m a.s.l.) is shown in Fig. 14.

22 **4.3 Independent evaluation**

24 Two methods are used to independently evaluate the tuned model.

- 25 1. The fraction (R^2_{adj}) of observed LSWT variance that is detected in the tuned model
26 is quantified; $inter_{\text{min}}$ and $inter_{\text{max}}$ (non-ice covered lakes) quantifies the observed
27 variance (K^2) in the month in which the minimum LSWT (var_{min}) and maximum
28 LSWT (var_{max}) occurs and $inter_{\text{jas}}$ (seasonally ice-covered lakes) quantifies the
29 observed variance (K^2) in the mean JAS LSWT (var_{jas}).

1 2. The metrics for 2011 (not used in tuning process) are compared with metrics from 2
2 tuned years.

4 **4.3.1 Variance detected in the tuned model**

5
6 The results show that the modelled LSWTs capture less of the true (observed) inter-annual
7 variance in lakes where the observed LSWT variance and the annual LSWT range is low.
8 This indicates that lower latitude lakes and high altitude lakes are less well simulated in the
9 model, than lakes with greater observed LSWT variance and annual range. This would also
10 indicate that lakes in the Southern Hemisphere at 35–55° S are less well simulated than
11 lakes in the Northern Hemisphere at the same latitude, as the annual LSWT range is
12 considerably lower at 35–55° S than at 35–55° N (Layden et al.,2015).

13
14 For non-ice covered temperate lakes, the $inter_{max}$ and $inter_{min}$ fraction is substantially
15 greater (0.49 and 0.37) than in tropical lakes (0.07 and 0.13), Table 9. This can be
16 explained by the greater observed variance (var_{max} and var_{min}) in temperate lakes (0.65 and
17 0.69 K²), than in tropical lakes (0.12 and 0.15 K²). Across all non-ice covered lakes var_{max}
18 and $inter_{max}$ show a correlation of 0.69 and var_{min} and $inter_{min}$ show a correlation of 0.33 (p
19 < 0.05), showing that lakes with greater observed variance have a greater portion of the
20 variance detected in the model. For high altitude seasonally ice-covered temperate lakes,
21 the fraction of the observed JAS LSWT inter-annual variance explained by the tuned
22 model is considerably less ($inter_{jas} = 0.21$) than for low altitude lakes (0.52), Table 9. The
23 variability in the observed JAS LSWT for high altitude lakes ($var_{jas} = 0.19$) is almost 4
24 times lower than for low altitude lakes (0.75). For seasonally ice-covered lakes the $inter_{jas}$
25 and var_{jas} are also correlated, 0.31, $p < 0.0005$. Furthermore, the annual range of monthly
26 LSWTs for non-ice covered lakes, explain 0.38 and 0.36 ($p < 0.0005$) of the variation in
27 var_{max} and var_{min} , with lakes of a low annual range (high altitude and tropical lakes),
28 showing less inter-annual variance. This supports the findings that tropical and high
29 altitude lakes are less well simulated in the model.

30

4.3.2 Comparison of tuned and untuned model LSWTS

The final year (2011) of available observational ARC-Lake LSWT data is used to independently evaluate the tuning process. The metrics from the tuned model forced for the year 2011 are compared with the metrics from two tuned years (1996; the first full year of data from ATSR2 and 2010; the last year of tuned data from Advanced ATSR (AATSR), as shown in Tables 10 and 11.

The mean metric results and the spread of differences across the 135 seasonally ice-covered lakes are highly comparable across all 3 years, with marginally better daily MAD metrics observed for the untuned year. For the 25 shallow lakes tuned with the modified tuning set-up, the MAD result for the untuned year is comparable with 2010. For the other 3 metrics, the untuned year has a lower spread of differences across lakes than those for 2010. The 1 °C warming day difference for the untuned year is greater than the difference for 2010 but less for 1996. The 1 °C cooling and warming day mean differences for 1996 and 2010 are less comparable for the 25 lakes than for the 135 lakes. This may be because the modelled effect of depth on the metrics is more predictable for deeper lakes, as illustrated in Fig. 15, than for shallow lakes.

Although inter-annual variance may somewhat obscure year-on-year comparisons, the results of the modelled LSWTs for the untuned year (2011) compare well to the modelled results from the tuned years (1996 and 2010) showing that the model remains stable when run with ERA forcing data outside the tuning period. For non-ice covered lakes, although the daily MAD and dispersion of errors is slightly higher for the untuned year, 2011, Table 11, overall, the metrics are very comparable to the metrics from 1996 and 2010.

5 Findings and discussion

5.1 The effect of the 1 °C warming day on JAS LSWT

Through the trial work, the modelled effect of a change in snow and ice albedo on the timing of 1 °C warming day (indicative of ice-off), the JAS LSWT and the timing of the 1 °C cooling day (indicative of ice-on) is demonstrated, for deep high latitude or very deep seasonally ice-covered lakes.

Using the default snow and ice albedo (α_1 , Table 2), the modelled 1 °C warming day of the 21 trial lakes occur, on average, 20 days too early. Across these lakes, a higher snow and ice albedo (α_2 , Table 2) results in a delay in the 1 °C warming day by 27 ± 12.6 days and a decrease in the JAS LSWT difference (between modelled and observed LSWTs) by ~50%, to 0.98 ± 2.51 °C. Much of the modelled variance in the JAS LSWT decrease, across the 21 lakes, is attributed to lake depth and latitude; accounting for 0.50 (R^2_{adj} , $p = 0.001$) of the variance (stepwise regression). Separately, depth accounts for 0.35 ($p = 0.003$) and latitude for 0.26 ($p = 0.01$) of the variance.

The LSWTs for 2 deep high latitude lakes (Great Bear and Great Slave) modelled with α_2 (high) and α_1 (low; default) snow and ice albedos, shown in Fig. 16, clearly shows the modelled effect of snow and ice albedo on the warming day and on the JAS LSWT. While the modelled change in the snow and ice albedo is the cause of the delay in the 1 °C warming day, we find that the decrease in the JAS LSWT for lakes with a delay of ~ 1 month in the 1 °C warming day is much greater for deep high latitude lakes, then for low latitude or shallow lakes. Great Slave (62° N and 41 m in depth) and Great Bear (66° N and 72 m in depth), show a 28 and 32 day delay in 1 °C warming day and a JAS LSWT decrease of 4.26 and 3.40 °C, while a delay of 29 and 32 days in the 1 °C warming day for Winnebago (44° N) and Khanka (45° N) both with depths of 5 m, showed only a small JAS LSWT decrease of ~0.1 °C. In Fig. 17, the lake-mean depth of the 21 trial lakes are plotted against latitude. The relationship between the depth and latitude of the lakes and the decrease in the JAS LSWT (presented as the decrease in the JAS LSWT, per week of

1 later 1 °C warming day, °C week⁻¹), is shown in this figure, by use of coloured circles. This
2 figure shows that for deep high latitude lakes the decrease in the JAS LSWT, is more
3 pronounced than for shallow low latitude lakes.

4
5 A study on Lake Superior (average depth of 147 m), shows a JAS LSWT warming trend
6 (of 2.5 °C from 1979 to 2006) substantially in excess of the air temperature warming trend
7 (Austin and Colman, 2007). Austin and Colman attribute this warming trend to a longer
8 warming period, caused by an earlier ice-off date, of ~0.5 day yr⁻¹. Foster and Heidinger
9 (2014) suggest warming trends in North America may be due to changes in cloud albedo;
10 with an observed loss of 4.2% in total cloudiness between 1982 and 2012.

11
12 As shown, the modelled decrease in the JAS LSWT (as a result of the higher albedo; α_2) is
13 more pronounced for deep lakes. The modelled 1 °C cooling day is also shown to occur
14 earlier in these lakes, with deeper lakes showing a greater earlier cooling. The 1 °C cooling
15 day occurs 3.4 days earlier for Great Slave, average depth of 41 m (decrease of 4.26 °C in
16 the modelled JAS LSWT). For Great Bear, average depth of 72 m, which shows a
17 modelled JAS LSWT decrease of 3.40 °C, has an earlier 1 °C cooling day, by 7.6 days.
18 The deepest lake in the trials, Lake Hovsgol, average depth of 138 m, shows a modelled
19 JAS LSWT decrease of 2.60 °C and an earlier 1 °C cooling day, by 12.8 days.

20
21 The findings are sensible. A delay in the 1 °C warming day, shortening the lake warming
22 period, may not prevent a shallow lake reaching its full heating capacity but may prevent a
23 deep lake from reaching its maximum heat storage capacity. At higher latitudes, the LSWT
24 warming period for northern hemispheric lakes becomes increasingly short (Layden et al.,
25 2015). As a result, deep lakes increasingly fall short of reaching their maximum heat
26 storage, causing a larger JAS LSWT decrease. Any changes to the 1 °C warming day of
27 deep and high latitude (or high altitude) lakes will therefore affect JAS LSWT. Deep lakes
28 also cool more slowly than shallow lakes, resulting in a later cooling day.

29
30 These findings highlight the sensitivity of the whole LSWT cycle of deep high latitude
31 lakes, to changes in snow and ice albedo and in the timing of the 1 °C warming day, as

1 illustrated in Fig. 15. This figure also illustrates how an earlier 1 °C cooling day caused by
2 a lower JAS LSWT may be counteracted or masked in deep lakes, where heat is retained
3 during the cooling period.

4
5 The effect that depth has on the JAS LSWT is apparent when comparing lakes at the same
6 altitude and latitude but with different depths. For example, Lake Nipigon and Lake
7 Manitoba, both located in Canada (50 °N and 51 °N) and at similar altitudes (283 m a.s.l.
8 and 247 m a.s.l) have considerably different depths, 55 m and 12 m respectively.
9 Significant differences are observed in JAS LSWT for these lakes, the deeper lake having
10 an average JAS LSWT 4.4 °C lower than that of the shallower lake (15.4 °C compared to
11 19.8 °C).

12
13 As the snow cover module with *FLake* is not operational in this version of the model; the
14 insulating effect that snow has on the underlying ice is not modelled. This may contribute
15 to the earlier 1 °C warming day and the higher JAS LSWTs, when modelled with the
16 default albedo. It is also possible that the icewater_flux value of 5 W/m² may be an
17 overestimation of the water-to-ice heat flux in the ice growth phase of deep and shallow
18 lakes. This greater heat flux, leading to underestimated ice thickness, could have
19 contributed to the large 1 °C warming day mean difference shown in table 5 (column 1). In
20 a study by Malm et al. (1997), the water-to-ice heat flux during the ice growth phase was
21 shown to be < 1 W/m² in both deep (15-20 m) and shallow lakes. Underestimated ice
22 thickness, causing an early ice melt, may possibly have led to over-tuning of albedo in the
23 tuned model.

24 25 26 **5.2 Lake-bottom temperatures modelled in *FLake***

27
28 The month of minimum LSWTs in the annual cycle (monthly minimum) have the potential
29 to be used as a proxy for determining the temperature of the bottom layer (hypolimnion) of
30 non-ice covered lakes. The monthly minimum climatological ARC-Lake LSWT explains
31 0.97 (R^2_{adj}) of the inter-lake variance in the bottom temperatures, obtained from the *FLake*

1 model based on the hydrological year 2005/2006 (Kirillin et al., 2011) and have a ~1:1
2 relationship, as shown in Fig. 18. Although *FLake* is a two-layer model; the depth of the
3 hypolimnion layer is not calculated, the bottom modelled temperature is representative of
4 the hypolimnion temperature, which remains constant with depth.

5
6 Empirically, it has previously been shown that from the equator to approximately 40°
7 (N/S), the steep decline in the minimum LSWT is reflected in the hypolimnion temperature
8 (Lewis, 1996). This relationship is applicable to deep stratified non-ice covered lakes. For
9 these lakes, the surface water, when at its coolest in the annual cycle (minimum LSWT)
10 and therefore its densest, sinks to the lake-bottom. During the summer stratification period,
11 the water in the upper mixed layer is warmer and less dense and therefore remains in the
12 upper layer (with exception to high wind or storm conditions, which can induce intense
13 vertical mixing). The strengthened density gradient in the summer thermocline (as
14 demonstrated for Lake Malawi in Fig. 4) also protects the hypolimnion from heat flux
15 through the lake surface. As a result, the lake hypolimnion temperature of deep non-ice
16 covered lakes can reflect the minimum LSWT. The comparability between the monthly
17 minimum LSWT (using the ARC-Lake monthly minimum climatology LSWTs) and the
18 bottom temperature, for all deep (> 25 m) non-ice covered lakes (14 lakes) supports this
19 empirical observation (Fig. 18).

20
21 In *FLake*, the bottom temperature is not independent of surface temperature; the change in
22 the surface heat flux over time is used in calculating the upper mixed layer temperature,
23 and the difference in heat flux between the upper mixed layer and lake-bottom are
24 considered in the lake-bottom temperature calculation (Kourzeneva and Braslavsky, 2005).
25 Although the minimum surface temperature is therefore related to the bottom temperature
26 in *FLake*, the good comparison between minimum ARC-Lake LSWTs and the bottom
27 temperatures, indicate that the monthly minimum LSWTs are a potential proxy for
28 determining the lake-bottom temperature. This also supports Lewis's empirical relationship
29 between lake surface temperature and lake-bottom temperature.

30
31 Although changes in other factors affect hypolimnion temperature, such as influx of cooler
32 water and geothermal heating, the monthly minimum LSWTs from satellites can offer a

1 good indication of hypolimnion temperature; useful in cases where this otherwise can not
2 be or is not observed directly.

4 **5.3 Wind speed scaling for low latitude lakes**

6 There is no optimal scaling for all non-ice covered lakes, as discussed in Sect. 3. This is
7 possibly attributable to the highly variable range of latitudes, LSWTs and mixing regimes
8 of non-ice covered lakes.

10 For the deep (> 25 m) non-ice covered lakes (14 lakes), the density difference between the
11 lake surface (in the month of maximum LSWT) and the hypolimnion during the summer
12 stratification period when the density (and temperature) gradient of the thermocline is
13 strongest, as illustrated in Fig. 4, was calculated (Haynes, 2013). For lakes at latitudes
14 below 35°N/S , the average density difference between these two layers is substantially
15 lower ($0.352 \times 10^{-3}\text{kg/m}^{-3}$) than for lakes at latitudes above 35°N/S ($1.183 \times 10^{-3}\text{kg/m}^{-3}$).
16 This is due to the smaller annual temperature range of the lower latitude lakes.

18 It is possible that the large density difference between the lake surface at maximum LSWT
19 and the hypolimnion in high latitude lakes during the stratification period, may produce a
20 buffer against wind induced mixing and therefore lessen the heat flux through the
21 thermocline. As winds can drive lake mixing in deep lakes, it strongly influences the mixed
22 layer depth and the LSWT. The larger the temperature (and density) gradient between the
23 lake surface and the hypolimnion during stratification, the more wind energy is required to
24 produce the same amount of mixing than for lakes with a smaller temperature (and density)
25 gradient between the two layers. Although the density differences between the two layers
26 are considered in *FLake*, the model is forced with over land wind speed measurements. It
27 is possible that when forced with an underestimated wind speed, the effect of wind on the
28 LSWT will be further reduced. As a result, higher latitude lakes may show more
29 representative LSWTs using a higher wind speed scaling.

1 **5.4 Improving modelled LSWTs in *FLake***

2
3 The optimal LSWT-regulating properties of the 244 lakes provide a guide to improving the
4 LSWT modelling in *FLake* for other lakes, without having to tune the model for each lake
5 separately.

6 7 **5.4.1 Depth**

8
9 The tuning results show that deep lakes are generally tuned to a shallower effective depth
10 and shallower lakes to a deeper effective depth. Figure 19 shows the relationship between
11 the lake-mean depth and the effective (tuned) depth of all 244 successfully tuned lakes,
12 colour coded by the effective depth factor optimised in the tuning process. The figure
13 legend shows that the effective depth factor decreases with increasing average lake depth
14 (also graphed in the figure insert), providing a means to estimate an appropriate effective
15 depth for any lake with a mean depth from 4–124 m.

16
17 The tuned lake depths are sensible. For shallow lakes, tuning to a deeper effective depth
18 may compensate for not having considered the ‘heat flux from sediments’ scheme in the
19 model. Retention of heat in the sediments of a lake has the same effect on modelled heat
20 storage capacity, as deepening the lake.

21
22 Many deep lakes have 3 distinct layers, the upper mixed layer, the underlying thermocline
23 and the bottom layer (hypolimnion), illustrated in Fig.4. As *FLake* is essentially a two-
24 layer model, it is possible that for deep lakes the mean depth (mean of entire lake depth) is
25 tuned to a shallower effective depth as it is more representative of the mean depth of the 2
26 upper lake layers. Other factors affecting the rate at which heat is exchanged between the
27 atmosphere and the surface water, such as topography, altitude, bathymetry and surface
28 area are not considered in *FLake*. It is possible that lake depth tuning may also compensate
29 for the effect that these factors have on the rate of the surface heat exchange.

30

5.4.2 Light extinction coefficient

Across all lakes, 57% were tuned to light extinction coefficient values of κ_{d4} or κ_{d5} . These lakes are globally distributed and have a wide range of mean depths (1-138 m) with an average mean depth of 16 m. In view of this finding and considering that light extinction coefficient values are scarce for the majority of lakes, we assess if κ_{d4} and κ_{d5} can be used to provide a good estimation of the light extinction coefficient for modelling LSWTs in *FLake*.

The untuned model is forced using two sets of light extinction coefficient values and the daily MAD results are compared. In the first model run, the average κ_{sd} value (derived from Secchi disk depth data) of the trial lakes of each lake type is applied to all lakes of corresponding type. For the 21 seasonally ice-covered trial lakes, $\kappa_{sd} = 0.82$; for the 14 non-ice covered trial lakes, $\kappa_{sd} = 1.46$. In the second run, the model is forced with κ_{d4} or κ_{d5} values. κ_{d4} is applied to all lakes > 16 m in depth (the average depth of lakes tuned with κ_{d4} or κ_{d5}) and κ_{d5} to all lakes < 16 m in depth. It makes practical sense to apply the less transparent of these two κ_d values (κ_{d5}) to shallower lakes, as shallow lakes are generally more affected by lake-bottom sediments than deeper lakes.

For both model runs the default albedo and the mean depth are applied, while all other model parameters are kept the same. A comparison of the two model runs shows that when LSWTs are modelled with κ_{d4} and κ_{d5} values, the daily MAD is reduced from 3.38 ± 2.74 to 2.28 ± 2.30 °C (33% decrease) across all lakes. This indicates that in the absence of available light extinction coefficient values, application of κ_{d4} and κ_{d5} values may improve the modelling of LSWTs of large lakes in *FLake*.

5.4.3 Snow and ice albedo

For seasonally ice-covered lakes, only 19% of the lakes were tuned to the default snow and ice albedo, α_1 , (snow and white ice = 0.60 and melting snow and blue ice = 0.10). Sixty four (64) % of lakes were tuned to two higher albedos α_2 or α_3 , (snow and white ice = 0.80 and melting snow and blue ice = 0.60 for α_2 or 0.40 for α_3), indicating that the default snow and ice albedo may be too low for the majority of lakes. In the absence of lake-specific snow and ice albedo information, the albedo value α_3 (snow and white ice = 0.80, melting snow and blue ice = 0.40) may provide a good estimate. The α_3 values are highly comparable to albedo values measured on a Lake in Minnesota using radiation sensors, where the mean albedo of new snow was shown to be 0.83 and the mean ice albedo (after snow melt) was 0.38 (Henneman and Stefan, 1999).

6 Summary and conclusions

The 1-dimensional freshwater lake model, *FLake*, was successfully tuned for 244 globally distributed large lakes (including saline and high altitude lakes) using observed LSWTs (ARC-Lake), for the period 1991 to 2010. This process substantially improves the measured mean differences in various features of the lake annual cycle, using only 3 lake properties (depth, snow and ice albedo and light extinction coefficient), as summarised in Table 5. In the process of tuning the model, we demonstrate several aspects of LSWT behaviour, in a way that cannot be done using the LSWT observations alone. We demonstrate the dependency of the whole modelled LSWT cycle of deep high latitude or high altitude lakes, on changes in the snow and ice albedo. The monthly minimum LSWTs from satellites are demonstrated to offer a good indication of the modelled lake-bottom temperature, with a 1:1 relationship shown (Fig. 18). This is highly useful where the lake-bottom temperature can not be or is not observed directly.

The amount of observed inter-annual LSWT variance (in the month in which the minimum LSWT and maximum LSWT occurs for non-ice covered lakes and in the JAS LSWT for

1 seasonally ice-covered lakes), detected in the tuned model was quantified. It can be
2 concluded that lakes where the observed LSWT variance is low (lower latitude and high
3 altitude) and for non-ice covered where the annual range is low are less well simulated in
4 the model, than lakes with greater observed LSWT variance and annual range.

5
6
7 We found that no wind speed scaling, uI , is most appropriate for lakes at lower latitudes, <
8 35° N/S, and that the largest scaling ($u3$; $U_{\text{water}} = 1.62 \text{ m/s} + 1.17U_{\text{land}}$), is most appropriate
9 for lakes at higher latitudes $> 35^\circ$ N/S. A greater resistance to wind induced mixing and
10 heat flux through the thermocline, as a result of a greater density gradient between the lake
11 surface and the hypolimnion of high latitude lakes, may explain the suitability of the
12 largest scaling to higher latitude lakes.

13
14 The optimal LSWT-regulating properties (effective depth, snow and ice albedo and light
15 extinction) for the 244 lakes are shown to be sensible and may provide a guide to
16 improving the LSWT modelling in *FLake* for other lakes, without having to apply a tuning
17 process to the model.

18
19 The relationship between the lake-mean depth and the effective (tuned) depth of all
20 244 successfully tuned lakes, show that deep lakes are generally tuned to a lower depth and
21 shallower lakes to a greater depth. Figure 19 provides a means to estimate an appropriate
22 effective depth for any lake with a mean depth from 4–124 m. An albedo value
23 $\alpha3$ (snow and white ice = 0.80, melting snow and blue ice = 0.40) is recommended in
24 place of the default value ($\alpha1$). Where κ values are unknown, applying κ_{d4} for lakes > 16 m
25 in depth and κ_{d5} for lakes < 16 m in depth improves the modelled LSWT.

26
27 This paper predominantly focused on the tuning of *FLake* and interpretation of the LSWT
28 annual cycle using the tuned model. The tuned model is forced with ERA data over the
29 available time span of LSWT observations (16–20 years) but has the potential to be forced
30 with ERA data covering a longer time span (ERA data are available for a period of > 33
31 years; 1979–2012). This offers the potential to provide a better representation of LSWTs

1 changes over a longer period of time, as satellite observations for the relatively short
2 period may reflect some inter-annual variance. As demonstrated, the use of remote sensing
3 and modelled LSWTs together extend the reliable quantitative details of lake behaviour
4 beyond the information from either remote sensing or models alone. The ARC-Lake
5 dataset has since been extended to include ~1000 smaller lakes (surface area > 100 km²)
6 worldwide, offering the potential to further quantify aspects of lake behaviour worldwide.

7
8 The findings in this study are expected to be of interest to limnologists concerned with the
9 relationship between certain features of the LSWT cycle and lake characteristics.
10 Limnologists may also benefit from other aspects of this study, for example, the effect of
11 wind speed scaling on LSWTs and how the observed minimum monthly LSWTs may be
12 used to estimate lake-bottom temperatures. The optimal LSWT-regulating properties of the
13 244 lakes may provide a guide to current and prospective users of *FLake* for improving the
14 LSWT modelling in *FLake* for other lakes, without having to tune the model for each lake
15 separately. This is of particular use for lakes where lake characteristic information is not
16 available. The described approach to this study can provide practical guidance to scientists
17 wishing to tune *FLake* to produce reliable LSWTs for new lakes.

18
19
20
21 Code availability

22 The code for the *FLake* model can be obtained from the following website; [http://www.
23 flake.igb-berlin.de/sourcecodes.shtml](http://www.flake.igb-berlin.de/sourcecodes.shtml)

24 Current Code Owner: DWD, Dmitrii Mironov

25 Phone: +49-69-8062 2705

26 Fax: +49-69-8062 3721

27 E-mail: dmitrii.mironov@dwd.de

28 History

29 Version: 1.00 Date: 17 November 2005

30 Modification comments:

1 In the MODULE *flake_parameters* where the values of empirical constants of the
2 lake model *FLake* and of several thermodynamic parameters are set, the ‘temperature
3 of maximum density of fresh water’, $t_{pl_T_r} = 277.13 \text{ K} (3.98 \text{ }^\circ\text{C})$.
4 In the SUBROUTINE *flake_driver* (*flake_driver.incf*), the model uses a number of
5 algorithms to update the bottom temperature, for example its relationship with mixed
6 layer depth. As *FLake* is intended for cold water lakes, if the bottom temperature shows
7 no relationship with the mixed layer depth, the models sets the lake-bottom temperature
8 to the temperatures of maximum density ($3.98 \text{ }^\circ\text{C}$). This creates a problem when modelling
9 tropical lakes; it causes the model to spin up to a wrong “attractor”. This problem
10 manifested itself in both the temperature profile and the mixed layer depth.
11 To overcome this problem, the lake-bottom temperature for non-ice covered lakes in
12 August (Southern Hemispheric winter), was used to set to the temperature of maximum
13 density, before compiling and running the model.
14
15 Language: Fortran 90. Software Standards: ‘European Standards for Writing and
16 Documenting Exchangeable Fortran 90 Code’.
17 The Supplement related to this article is available online at
18 [doi:10.5194/gmdd-8-8547-2015-supplement](https://doi.org/10.5194/gmdd-8-8547-2015-supplement).
19
20 *Author contributions.* A. Layden developed and applied the tuning methodology and code,
21 accessed all meteorological and LSWT data, performed the data analysis and prepared the
22 manuscript. S. MacCallum derived the ARC-Lake LSWT observations and provided
23 technical support. C. Merchant initiated the ARC-Lake project and supervised the work in
24 this study.
25
26 *Acknowledgements.* The authors gratefully acknowledge that this work is funded by the
27 European Space Agency under contract 22184/09/I-OL.
28 The authors also gratefully acknowledge Georgiy Kirillin, the author of *FLake* lake model.

1 **References**

- 2 Armengol, J., Caputo, L., Comerma, M., Feijoó, C., García, J. C., Marcé, R., Navarro, E.,
3 and Ordoñez, J.: Sau reservoir's light climate: relationships between Secchi depth and light
4 extinction coefficient, *Limnetica*, 22, 195–210, 2003.
- 5
- 6 Ashton, G. D.: *River and Lake Ice Engineering*, Water Resources Publication, Littleton,
7 CO, 355 pp., 1986.
- 8
- 9 Austin, J. A. and Colman, S. M.: Lake Superior summer water temperatures are increasing
10 more rapidly than regional air temperatures: a positive ice-albedo feedback, *Geophys. Res.*
11 *Let.*, 34, L06604, doi:10.1029/2006GL029021, 2007.
- 12
- 13 Bernhardt, J., Engelhardt, C., Kirillin, G., and Matschullat, J.: Lake ice phenology in
14 Berlin-Brandenburg from 1947–2007: observations and model hindcasts, *Climatic Change*,
15 112,791–817, 2012.
- 16
- 17 Brown, L. C. and Duguay, C. R.: The response and role of ice cover in lake-climate
18 interactions, *Prog. Phys. Geog.*, 34, 671–704, doi:10.1177/0309133310375653, 2010.
- 19
- 20 Bukata, R. P., Jerome, J. H., and Bruton, J. E.: Relationships among secchi disk depth,
21 beam attenuation coefficient, and irradiance attenuation coefficient for great-lakes waters,
22 *J. Gt. Lakes Res.*, 14, 347–355, doi:10.1016/S0380-1330(88)71564-6, 1988.
- 23
- 24 Dee, D. P., Uppala, S. M., Simmons, A. J., et al.: The ERA-Interim reanalysis:
25 configuration and performance of the data assimilation system, *Q. J. Roy. Meteor. Soc.*,
26 137, 553–597, doi:10.1002/qj.828, 2011.
- 27
- 28 Dutra, E., Stepanenko, V. M., Balsamo, G., Viterbo, P., Miranda, P. M. A., Mironov, D.,
29 and Schaer, C.: An offline study of the impact of lakes on the performance of the ECMWF
30 surface scheme, *Boreal Environ. Res.*, 15, 100–112, 2010.
- 31
- 32 ECMWF: European Centre for Medium-Range Weather Forecasts. ECMWF ERAInterim
33 Re-Analysis data, [Internet], NCAS British Atmospheric Data Centre, September
34 2009–November 2012, available at: [http://badc.nerc.ac.uk/view/badc.nerc.ac.uk__](http://badc.nerc.ac.uk/view/badc.nerc.ac.uk__ATOM__dataent_1245854315822775)
35 [_ATOM__dataent_1245854315822775](http://badc.nerc.ac.uk/view/badc.nerc.ac.uk__ATOM__dataent_1245854315822775) (last access: November 2012), 2009.
- 36
- 37 Foster, M., and Heidinger, A.: PATMOS-x: Results from diurnally corrected 30-yr satellite
38 cloud climatology. *J. Climate*, 26, 414–425, doi:10.1175/JCLI-D-11-00666.1, 2014
- 39
- 40 Haynes, W. M.: *CRC Handbook of Chemistry and Physics*, 94th Edn., Taylor & Francis
41 Limited, Florida, USA, 2013.
- 42

- 1 Henneman, H. E. and Stefan, H. G.: Albedo models for snow and ice on a freshwater lake,
2 Cold Reg. Sci. Technol., 29, 31–48, 1999.
- 3
- 4 Herdendorf, C. E.: Large Lakes of the World, J. Gt. Lakes Res., 8, 379–412, 1982.
- 5
- 6 Holmes, R. W.: Secchi disk in turbid coastal waters, Limnol. Oceanogr., 15, 688–694,
7 1970.
- 8
- 9 Hsu, S. A.: Coastal Meteorology, Academic Press Inc., San Diego, USA, 1988.
- 10 ILEC: World Lake Database, International Lake Environment Committee Foundation,
11 available at: <http://wldb.ilec.or.jp> (last access: May 2011), 1999.
- 12
- 13 Jerlov, N. G.: Marine Optics, Elsevier Scientific Publishing Company, Amsterdam, the
14 Netherlands, 1976.
- 15
- 16 Kirillin, G., Hochschild, J., Mironov, D., Terzhevik, A., Golosov, S., and Nutzmann, G.:
17 *FLake*-Global: online lake model with worldwide coverage, Environ. Modell. Softw., 26,
18 683–684, 2011.
- 19
- 20 Kourzeneva, E., Asensio, H., Martin, E., and Faroux, S.: Global gridded dataset of lake
21 coverage and lake depth for use in numerical weather prediction and climate modelling,
22 Tellus A, 64, 15640, doi:10.3402/tellusa.v64i0.15640, 2012.
- 23
- 24 Kourzeneva, K., and Braslavsky, D.: Lake model *FLake*, coupling with atmospheric
25 model: first steps. Proc. of the 4th SRNWP/HIRLAM Workshop on Surface Processes
26 and Assimilation of Surface Variables jointly with HIRLAM Workshop on Turbulence, S.
27 Gollvik, Ed., SMHI, Norrkoping, Sweden, 43-54, 2005
- 28
- 29 LakeNet: LakeNet's Global Lake Database, available at: <http://www.worldlakes.org> (last
30 access: May 2011), 2003.
- 31
- 32 Lane, D. M.: Online Statistics Education: A Multimedia Course of Study
33 (<http://onlinestatbook.com/>), Rice University. (last access: Mar 2016)
- 34
- 35 Launiainen, J. and Cheng, B.: Modelling of ice thermodynamics in natural water bodies,
36 Cold Reg. Sci. Technol., 27, 153–178, 1998.
- 37
- 38 Layden, A., Merchant, C. and MacCallum, S.: Global climatology of surface water
39 temperatures of large lakes by remote sensing, Int. J. Climatol., doi:10.1002/joc.4299,
40 online first, 2015.
- 41
- 42 Lehner, B. and Döll, P.: Development and validation of a global database of lakes,
43 reservoirs and wetlands, J. Hydrol., 296, 1–22, doi:10.1016/j.jhydrol.2004.03.028, 2004.
- 44

1 Lerman, A., Imboden, D., and Gat, J.: Physics and Chemistry of Lakes, Verlag Springer,
2 Berlin, Heidelberg, 1995.
3

4 Lewis Jr., W. M.: Tropical lakes: how latitude makes a difference, in: Perspectives in
5 Tropical Limnology, edited by: Schiemer, F. and Boland, K. T., SPB Academic Publishers,
6 Amsterdam, the Netherlands, 43–64, 1996.
7

8 Long, Z., Perrie, W., Gyakum, J., Caya, D., and Laprise, R.: Northern lake impacts on
9 local seasonal climate, *J. Hydrometeorol.*, 8, 881–896, 2007.
10

11 MacCallum, S. N. and Merchant, C. J.: Surface water temperature observations of large
12 lakes by optimal estimation, *Canadian Journal of Remote Sensing*, 38, 25–45,
13 doi:10.5589/m12-010, 2012.
14

15 Malm, J., Terzhevik, A., Bengtsson, L., Boyarinov, P., Glinsky, A., Palshin, N. and Petrov
16 M.: Temperature and salt content regimes in three shallow ice-covered lakes: 2. Heat and
17 mass fluxes, *Nordic Hydrol.*, 28, 129-152, 1997
18

19 Mironov, D. V.: Parameterization of lakes in numerical weather prediction, description of a
20 lake model, German Weather Service, Offenbach am Main, Germany, 2008.
21

22 Mironov, D., Heise, E., Kourzeneva, E., Ritter, B., Schneider, N. and Terzhevik, A.:
23 Implementation of the lake parameterisation scheme *FLake* into the numerical weather
24 prediction model COSMO. *Boreal Env. Res.* 15, 218-230, 2010
25

26 Mironov, D., and Ritter, B.: Testing the new ice model for the global NWP system GME
27 of the German Weather Service. *Research Activities in Atmospheric and Oceanic*
28 *Modelling*, J. Cote, Ed., Report No. 34, April 2004, WMO/TD-No. 1220, 4.21-4.22, 2004.
29

30 Monson, B.: A Primer on Limnology, Water Resources Center, University of Minnesota,
31 St Paul, MN, 1992.
32

33 Poole, H. H. and Atkins, W. R. G.: Photo-electric measurements of submarine illumination
34 throughout the year, *Jour Marine Biol Assoc United Kingdom*, 16, 297–324, 1929.
35

36 Pour, H. K., Duguay, C. R., Martynov, A., and Brown, L. C.: Simulation of surface
37 temperature and ice cover of large northern lakes with 1-D models: a comparison with
38 MODIS satellite data and in situ measurements, *Tellus A*, 64, 17614,
39 doi:10.3402/tellusa.v3464i3400.17614, 2012.
40

41 Resio, D. T., Bratos, S. M., and Thompson, E. F.: Meteorology and Wave climate, in:
42 *Coastal Engineering Manual*, chapter II-2. U.S. Army Corps of Engineers. Washington,
43 DC, USA, 2003.
44

1 Rooney, G. G., and Jones, I. D.: Coupling the 1-D lake model *FLake* to the community
2 land-surface model JULES. *Boreal Env. Res.*, **15**, 501-512, 2010.
3
4 Sherwood, I.: On the Universality of the Poole and Atkins Secchi Disk-light Extinction
5 Equation, U.S. Water Conservation Lab, Phoenix, Arizona 85040, USA, 1974.
6
7 Sousounis, P.J., and Fritsch, J.M.: Lake-aggregate mesoscale disturbances. Part II: A case
8 study on the effects on regional and synoptic-scale weather systems, *Bull. Amer. Meteor.*
9 *Soc.*, 75,1793-1811, 1994.
10
11 Voros, M., Istvanovics, V., and Weidinger, T.: Applicability of the *FLake* model to Lake
12 Balaton, *Boreal Environ. Res.*, 15, 245–254, 2010.
13
14 Walker, G.A., and Shostak, J.: *Common Statistical Methods for Clinical Research with*
15 *SAS® Examples*, Third Edition. Cary, NC: SAS Institute Inc, 2010.
16
17

Tables

ERA data components and description	<i>FLake</i> input
SSRD (shortwave solar downward radiation); 3 hourly SSRD, cumulative over 12 hour forecasts (W/m^2)	Mean daily SSRD W/m^2
T2; 6 hourly air temperature at 2 metres (K)	Mean daily T2 ($^{\circ}\text{C}$)
D2; 6 hourly dewpoint at 2 metres (K),	Mean daily vapour pressure (hPa) $= P(z) * 10^{(7.5(\text{dewpoint} / (237.7 + \text{dewpoint})))}$ Where $P(z) = P(\text{sea level}) * \exp(-z/H)$. $P(z)$ = pressure at height z , $P(\text{sea level})$ = sea level pressure (~ 1013 mb), z = height in metres, H = scale height (~ 7 km) http://www.gorhamschaffler.com/humidity_formulas.htm
U10 and V10; 6 hourly wind components at 10 meters (m/s)	Mean daily wind speed (m/s); $= \text{sqrt}(V10^2 + U10^2)$ U component represents eastward wind (west to east wind direction) V component represents northward wind (south to north wind direction)
TCC (total cloud cover); 6 hourly TTC	Mean daily TCC

Table 1 ECMWF Interim Re-analysis (ERA) data components and *FLake* input format

Effective depth factors (Z_d)	Light extinction coefficient (κ_d)				albedo (α)	Snow & white ice Albedo	Melting snow & blue ice albedo
	κ_d	375nm	475nm	700nm			
Z_{d1}	κ_{d1}	0.038	0.018	0.56	$\alpha1$	0.60	0.10
	κ_{d2}	0.052	0.025	0.57	$\alpha2$	0.80	0.60
Z_{d2} ($Z_{d1} * 0.75$)	κ_{d3}	0.066	0.033	0.58	$\alpha3$	0.80	0.40
Z_{d3} ($Z_{d1} * 0.5$)	κ_{d4}	0.122	0.062	0.61	$\alpha4$	0.60	0.30
Z_{d4} ($Z_{d1} * 1.5$)	κ_{d5}	0.22	0.116	0.66			
	κ_{d6}	0.80	0.17	0.65			
Z_{d5} ($Z_{d1} * 0.3$)	κ_{d7}	1.10	0.29	0.71			
Z_{d6} ($Z_{d1} * 2.5$)	κ_{d8}	1.60	0.43	0.80			
Z_{d7} ($Z_{d1} * 2.0$)	κ_{d9}	2.10	0.71	0.92			
Z_{d8} ($Z_{d1} * 4.0$)	κ_{d10}	3.00	1.23	1.10			

Table 2 Effective depth factors (Z_d), light extinction coefficient values (κ_d) and snow and ice albedo values (α) used in tuning study. Eighty (80) possible combinations used for tuning of seasonally ice-covered lakes ($Z_{d1} : Z_{d4} \times \kappa_{d1} : \kappa_{d5} \times \alpha1 : \alpha4$). The modified tuning for the 25 shallow seasonally ice-covered lakes utilised greater depth factors; $Z_{d6} : Z_{d8}$ and 2 higher light extinction coefficient values, κ_{d6} and κ_{d7} . Sixty (60) possible combinations used for tuning of non-ice covered lakes ($Z_{d1} : Z_{d6} \times \kappa_{d1} : \kappa_{d10}$). The spectre for the 10 κ_d values are divided (in fractions of 0.18, 0.54, 0.28) into three wavelengths: 375, 475 and 700nm, respectively.

LSWT-regulating properties	Effect on metric	Metrics (mean differences between observed and modelled LSWTs)
κ (light extinction coefficient)	κ affects irradiance transmission of surface water, which is more notable in summer months.	JAS LSWT mean difference ($^{\circ}\text{C}$) $= (\bar{x}_i^{mod_jas} - \bar{x}_i^{obs_jas})$ mod_jas = modelled JAS LSWT obs_jas = observed JAS LSWT
d (depth)	d alters heat storage capacity affecting timing of the start of the cold phase (the day that the LSWT drops to below 1°C)	1°C cooling day mean difference (days)
α (snow and ice albedo)	α alters ice/snow reflectance affecting the end of the cold phase (the day that the LSWT increases to above 1°C)	1°C warming day mean difference (days)
d, α and κ	All LSWT-regulating properties contribute to the comparability of the modelled and observed LSWT	Daily MAD ($^{\circ}\text{C}$) $= \sum (\text{abs}(x_i^{mod} - x_i^{obs})) / N;$ mod = daily modelled LSWTs obs = daily observed LSWTs N = sample size

Table 3 Relationship between the Lake Surface Water Temperature (LSWT) regulating properties and metrics, showing the equations for determining the daily mean absolute difference (MAD) and the July, August, September (JAS) LSWT mean difference

Trial results for untuned model							
Seasonally ice-covered trial lakes (21 lakes)				Non-ice covered lakes (14 lakes)			
Metrics	u1	u2	u3	Metrics	u1	u2	u3
daily MAD (°C) (mean absolute difference)	3.07 ±2.25	2.66 ±1.93	2.02 ±1.30	daily MAD (°C)	3.55 ±3.20	3.11 ±2.77	2.17 ±1.93
Mean JAS (July August September) LSWT mean difference (°C)	3.71 ±3.51	3.07 ±3.41	1.87 ±2.93	mth_{max} (°C) (mean difference between observed and modelled LSWTs for the month of maximum observed LSWT)	1.92 ±5.05	1.39 ±5.06	-0.42 ±5.18
1 °C cooling day (the day the lake- mean LSWT drops to below 1 °C) mean difference (days)	12.0 ±39.6	7.9 ±33.3	1.0 ±30.5	mth_{min} (°C) (mean difference between observed and modelled LSWTs for the month of minimum observed LSWT)	3.71 ±4.33	3.08 ±4.16	1.47 ±3.87
1 °C warming day (the day the lake- mean LSWT rises to above 1 °C) mean difference (days)	- 27.1 ±29.7	- 23.6 ±22.7	- 20.3 ±18.4				

Table 4 The effect of wind speed scaling on untuned modelled LSWTs, presented as the mean difference, between the modelled and observed values, across lakes with the spread of differences defined as 2σ , where wind speeds $u1$ is unscaled, $u2$ is factored by 1.2 and $u3$ ($U_{water} = 1.62 \text{ m/s} + 1.17U_{land}$). Results are presented for seasonally ice-covered and non-ice covered trial lakes. Results highlight that $u3$ is most applicable to seasonally ice-covered lakes but there is no one wind speed most suited for all lakes (While the mean difference is improved with $u3$, the spread of the mean differences across lakes for mth_{min} and mth_{max} show little change).

Seasonally ice-covered lakes				Non-ice covered lakes			
metrics	Untuned (21 trial lakes)	Tuned (21 trial lakes)	Tuned (160 lakes)	Metrics	Untuned (14 trial lakes)	Tuned (14 trial lakes)	Tuned (84 lakes)
daily MAD (°C)	3.07 ±2.25	0.84 ±0.51	0.80 ±0.56	daily MAD (°C)	3.55 ±3.20	0.96 ±0.63	0.96 ±0.66
Mean JAS LSWT mean difference (°C)	3.71 ±3.51	-0.12 ±1.09	-0.06 ±1.15	mth_{max} (°C)	1.92 ±5.05	-0.44 ±1.52	-0.21 ±1.47
1 °C cooling day mean difference (days)	12.0 ±39.6	-1.6 ±12.8	-1.08 ± 8.5	mth_{min} (°C)	3.71 ±4.33	-0.03 ±1.48	-0.08 ±1.47
1 °C warming day mean difference (days)	- 27.1 ±29.7	-0.2 ±10.7	0.3 ±12.3				

Table 5 Summary of the untuned and tuned metrics for the trial lakes and the tuned metrics for all lakes (metrics are explained in Table 4). The results, presented for seasonally ice-covered and non-ice covered lakes in each instance, show the mean between the modelled and observed values, across lakes with the spread of differences defined as 2σ . For tuned lakes, wind speed scaling u^3 was applied to all seasonally ice-covered and to non-ice covered lakes $> 35^\circ\text{N/S}$ and no scaling ($u1$) to non-ice covered lakes $< 35^\circ\text{N/S}$.

Tuning metrics	135 lakes	25 lakes (modified tuning)	All lakes (160)	Trial lakes
daily MAD (°C)	0.74± 0.48	1.11± 0.56	0.80± 0.56	0.84± 0.51
Mean JAS mean difference (°C)	-0.01± 1.11	- 0.34±1.22	-0.06± 1.15	-0.12± 1.09
1 °C cooling day mean difference (days)	-1.0± 8.8	-1.3± 6.9	-1.08± 8.5	-1.6 ± 12.8
1 °C warming day mean difference (days)	0.5± 12.6	- 0.5± 10.2	0.3± 12.3	-0.2± 10.7

Table 6 Comparison of metric results for seasonally ice-covered lakes: 135 lakes tuned using the initial tuned setup for seasonally ice-covered lakes (Table 2), 25 lakes tuned with the modified set-up (Table 2), all lakes, and trial lakes. The spread of differences across lakes is defined as 2σ . The metrics are explained in Table 4.

Tuned metrics	Tuned results for 160 seasonally ice-covered lakes			
	Saline (37 lakes)	Freshwater (123 lakes)	Altitude >3200 m a.s.l. (14 lakes)	Altitude < 2000 m a.s.l. (146 lakes)
daily MAD (°C)	0.90± 0.69	0.76± 0.50	0.61± 0.24	0.81± 0.57
Mean JAS mean difference (°C)	-0.23± 1.14	-0.01± 1.14	0.06± 1.14	-0.07± 1.15
1 °C cooling day mean difference (days)	-1.3± 9.7	-1.0± 8.3	-3.1± 10.8	-0.9± 8.2
1 °C warming day Mean difference (days)	0.0± 13.1	0.4± 12.0	0.9± 13.6	0.3± 12.1

Table 7 Comparison of tuned model results for saline, freshwater, high and low altitude seasonally ice-covered lakes, with the spread of differences across lakes, 2σ . The metrics are explained in Table 4.

Tuned metrics	Tuned results for 84 non-ice covered lakes			
	Saline (26 lakes)	Freshwater (58 lakes)	Altitude > 1500 m a.s.l. (10 lakes)	Altitude < 1500 m a.s.l. (74 lakes)
daily MAD (°C)	1.06 ±0.67	0.91 ±0.64	1.03 ±0.82	0.95 ±0.64
$mith_{max}$ (°C)	-0.31 ±1.90	-0.16 ±1.24	-0.40 ±2.12	-0.18 ±1.37
$mith_{min}$ (°C)	-0.25 ±1.74	-0.01 ±1.33	-0.14 ±1.30	-0.07 ±1.50

Table 8 Comparison of tuned metric results for saline, freshwater and high and low altitude non-ice covered lakes, with the spread of differences across lakes, 2σ . The metrics are explained in Table 4.

Non-ice covered lakes	All lakes (84)	Temperate lakes > 20° N/S (44 lakes)	Tropical lakes < 20° N/S (40 lakes)
$var_{\max} (K^2)$ the inter-annual variance in the mean LSWT observations for the month of maximum LSWT	0.40	0.65	0.12
$inter_{\max} (R^2_{\text{adj}})$ The fraction of the observed variances (var_{\max}) accounted for in the tuned model	0.29 ± 0.63	0.49 ± 0.58	0.07 ± 0.31
$var_{\min} (K^2)$ the inter-annual variance in the mean LSWT for the month of minimum LSWT	0.43	0.69	0.15
$inter_{\min} (R^2_{\text{adj}})$ The fraction of the observed variances (var_{\min}) accounted for in the tuned model	0.25 ± 0.49	0.37 ± 0.49	0.13 ± 0.37
Seasonally ice-covered lakes	All lakes (160)	Altitude > 3200 m a.s.l. (14 lakes)	Altitude < 2000 m a.s.l. (146 lakes)
$var_{\text{jas}} (K^2)$ the inter-annual variance in the mean JAS LSWT	0.70	0.19	0.75
$inter_{\text{jas}} (R^2_{\text{adj}})$ The fraction of the observed variances (var_{jas}) accounted for in the tuned model	0.50 ± 0.62	0.21 ± 0.46	0.52 ± 0.59

Table 9 The fraction (R^2_{adj}) of observed inter-annual variance detected in the model. Maximum and minimum LSWT is used for non-ice covered lakes ($inter_{\max}$ and $inter_{\min}$), while July, August and September (JAS) LSWT is used for seasonally ice-covered lakes, ($inter_{\text{jas}}$). This table highlights that where the observed inter-annual variance is low, the proportion of variance detected in the model is also low (high altitude seasonally ice-covered lakes and tropical lakes).

Tuned metrics	135 lakes			25 lakes (modified tuning set-up)		
	2011 Untuned	1996 Tuned (ATSR2)	2010 Tuned (Advanced ATSR)	2011 Untuned	1996 Tuned (ATSR2)	2010 Tuned (Advanced ATSR)
daily MAD (°C)	0.86±0.68	0.89±0.74	0.87±0.71	1.59±1.04	1.33±0.79	1.66±0.95
Mean JAS mean difference (°C)	0.18±1.50	-0.33±1.79	0.28±1.44	0.12±1.71	0.17±1.19	0.28±1.81
1 °C cooling day mean difference (days)	11.1±23.8	5.1±25.6	8.5±21.4	10.9±18.7	-3.0±41.9	11.7±31.3
1 °C warming day mean difference (days)	7.4±19.7	12.1±19.7	6.5±19.8	9.33±21.6	13.2±18.2	1.0±32.54

Table 10 Results of independent evaluation of the tuning process for seasonally ice-covered lakes. The spread of differences across lakes is defined as 2σ . These results illustrate that the metrics (explained in Table 4) from the untuned year (2011) compare well with metrics from 1996 (the first full year of data from Along-Track Scanning Radiometers 2 (ATSR2) and 2010 (the last year of tuned data from Advanced ATSR. For the untuned year (2011), for each lake, the model is forced with the effective lake depth (Z_d), snow and ice albedo (α) and light extinction coefficient (κd) values determined during the tuning process, shown in the supplement.

Tuned Metrics	2011 Untuned	1996 Tuned (ATSR2)	2010 Tuned (Advanced ATSR)
daily MAD (°C)	1.07±0.91	0.98±0.82	0.97±0.81
mth_{max} (°C)	-0.23±2.40	-0.32±1.86	-0.31±2.20
mth_{min} (°C)	-0.02±2.04	-0.23±1.73	+0.11±2.15

Table 11 Results of the independent evaluation of the tuning process for non-ice covered lakes. The spread of differences across lakes is defined as 2σ . Metrics (explained in Table 4) for the untuned year (2011) are compared with those from the first full year of data from Along-Track Scanning Radiometers 2 (ATSR2) (1996) and the last year of tuned data from Advanced ATSR (2010). For the untuned year (2011), for each lake, the model is forced with the effective lake depth (Z_d), snow and ice albedo (α) and light extinction coefficient (κ_d) values determined during the tuning process, shown in the supplement.

Figures

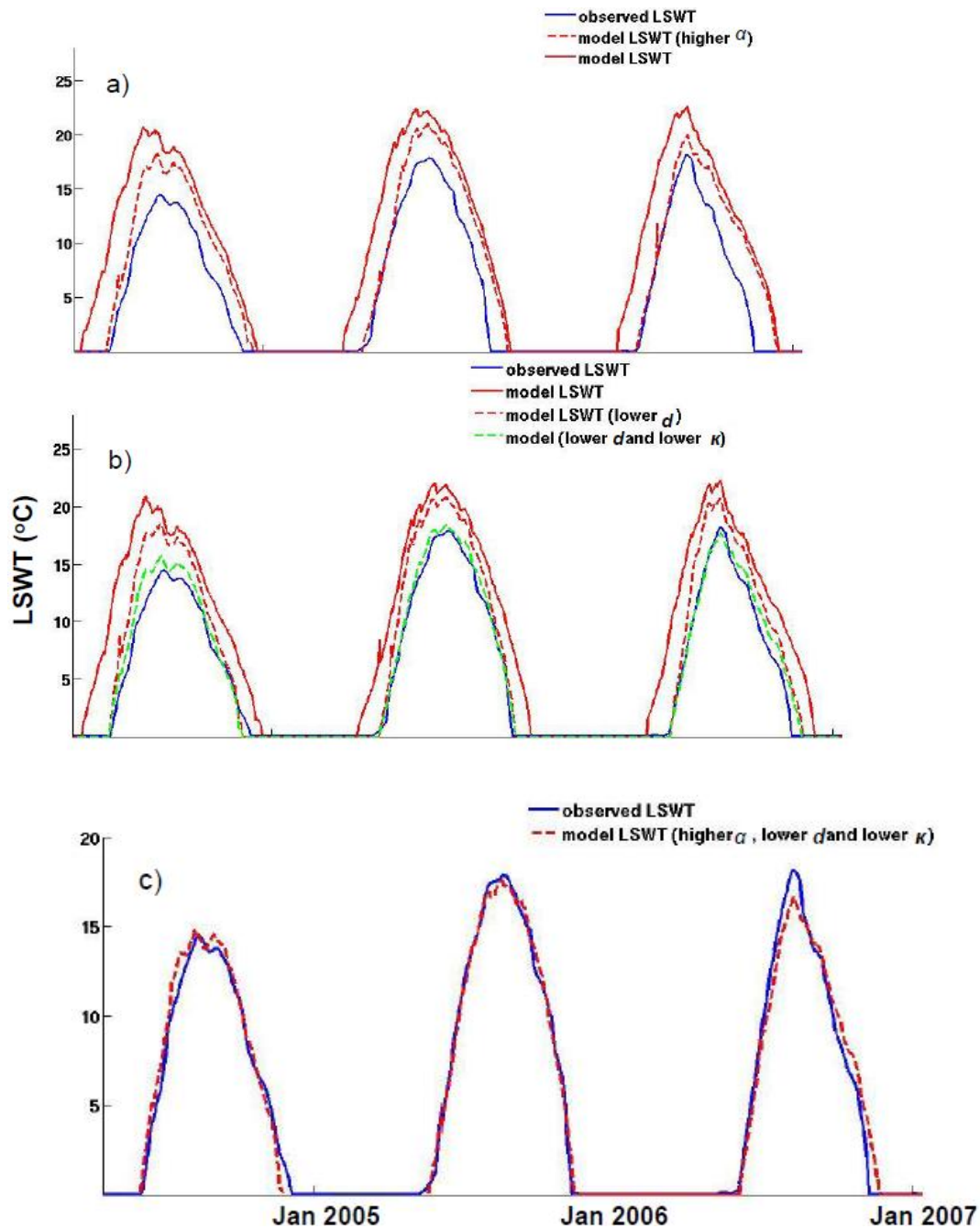


Figure 1 Preliminary modelled runs for Lake Athabasca, Canada (59° N 110° W), showing that adjustments to lake depth (d), snow and ice albedo (α) and light extinction coefficient (κ) can greatly improve the modelled lake surface water temperatures (LSWTs) compared to the default/ recommended d , α and κ values; a) shows that a higher α causes a later ice-off date, comparing well with the observed (ARC-Lake) ice-off date, b) shows that a lower d causes an earlier ice-on date and a lower κ value (greater transparency) reduces the maximum LSWT and c) shows that the combined effect of the adjusted d , α and κ produce LSWTs that are highly comparable to the observed ARC-Lake LSWTs.

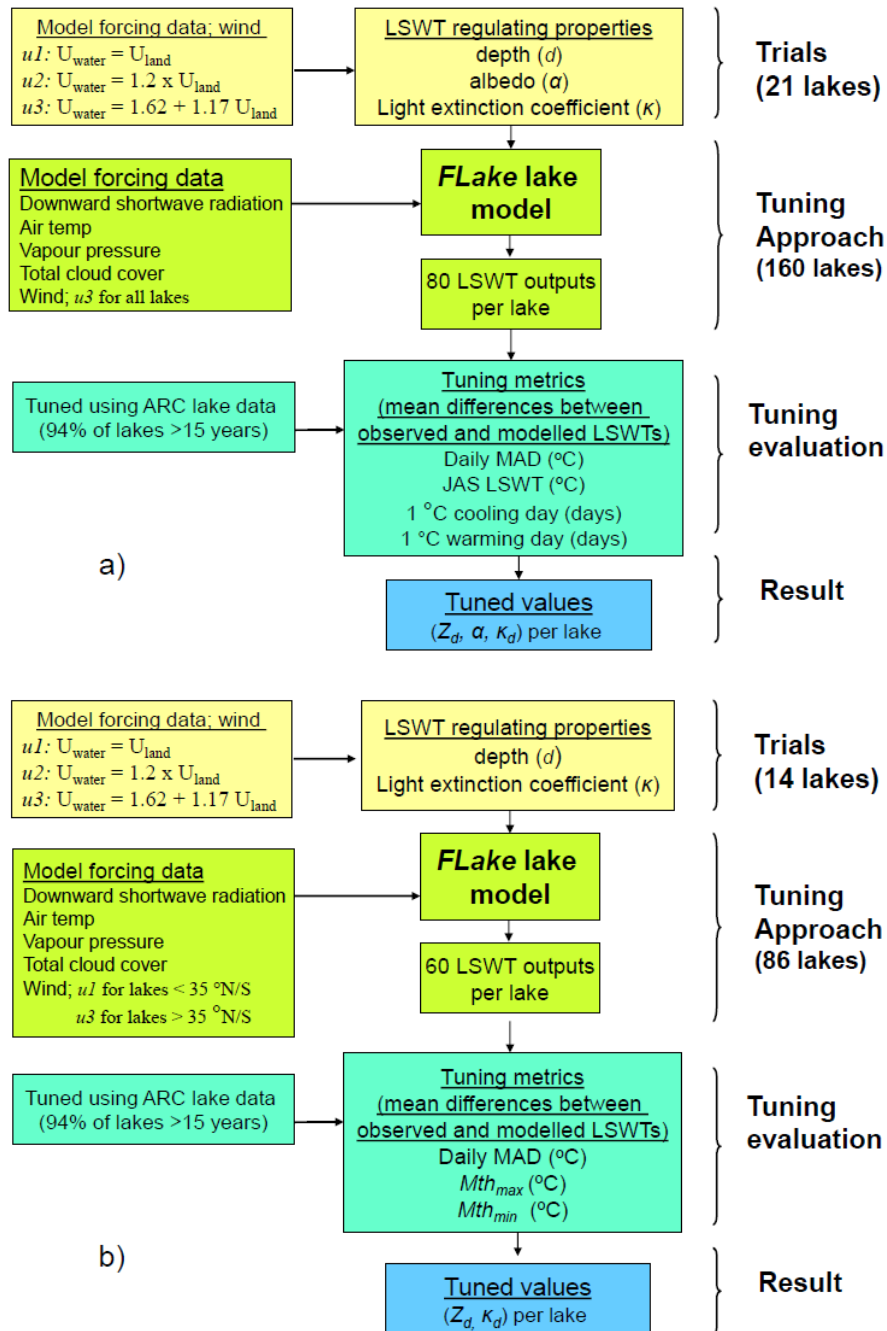


Figure 2 Study approach overview (trials, tuning, evaluation and results) for a) seasonally ice-covered lakes and b) non-ice covered lakes. For the trials, wind speed scaling, $u1$, $u2$ (recommended for lakes with fetch > 16 km and $u3$ (recommended for open ocean water) is assessed on the untuned model, tuning is then trialed with a range of factors for d and values for α and κ using the selected wind speed scaling. The tuning approach produces modelled LSWTs for all possible combination of d , α and κ , 80 modelled runs for seasonally ice-covered lakes and 60 for non-ice covered lakes. For the evaluation, the tuning metrics (normalized and equally weighted) are the basis for selection of the optimal (tuned) LSWT model for each lake.

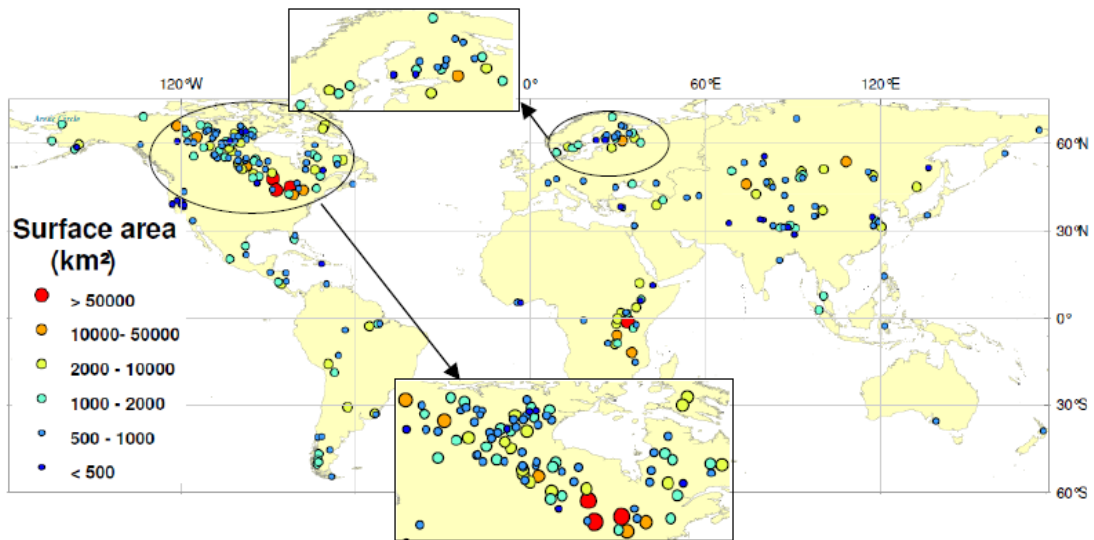


Figure 3 Location of 246 observed lakes colour coded by surface area (obtained using polygon area in Global Lakes and Wetlands Database (GLWD) showing zoomed inset of North America and Northern Europe.

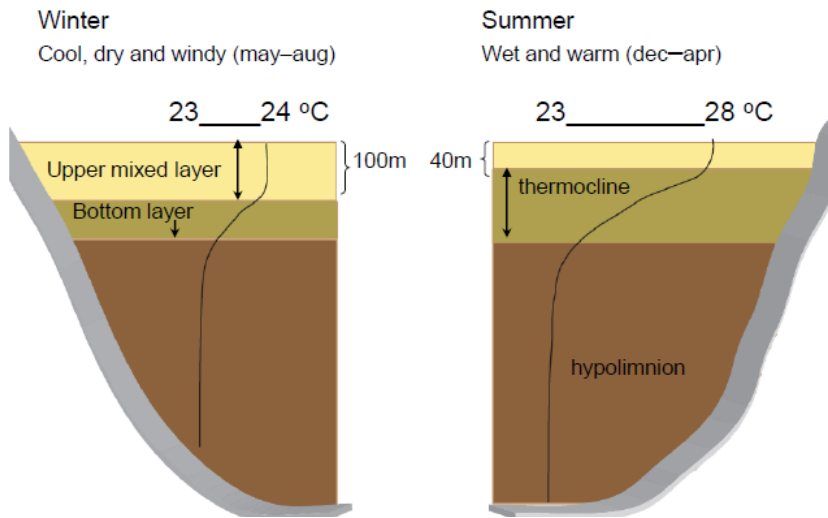


Figure 4 Winter and summer depth and temperature profile for Lake Malawi (mean depth of 273 m), Africa ($12^{\circ}\text{S } 35^{\circ}\text{E}$), illustrated using data from the ILEC world lake database (<http://wldb.ilec.or.jp/>); showing the three distinct layers (in winter and summer) of a deep stratified non-ice covered lake. *FLake*, a two-layer model, predicts the depth and temperature of the ‘upper mixed layer’ and the temperature of the ‘bottom layer’ (shown on the left), and ‘thermocline’ depth and temperature profile (shown on the right).

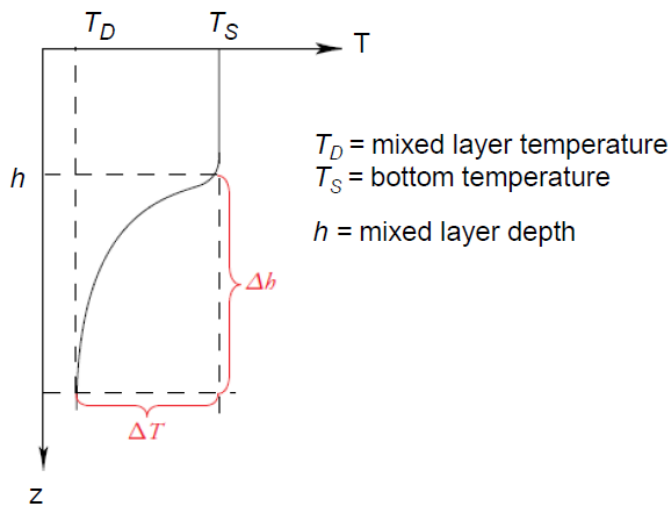


Figure 5 Schematic representation of the temperature profile in the upper mixed layer and in the thermocline, reproduced from Killirin (2003). The self-similarity representation of the temperature profile in *FLake* is determined using dimensionless co-ordinates, $\zeta = (z-h)/\Delta h$, and $v = [T(z)-T_D]/\Delta T$.

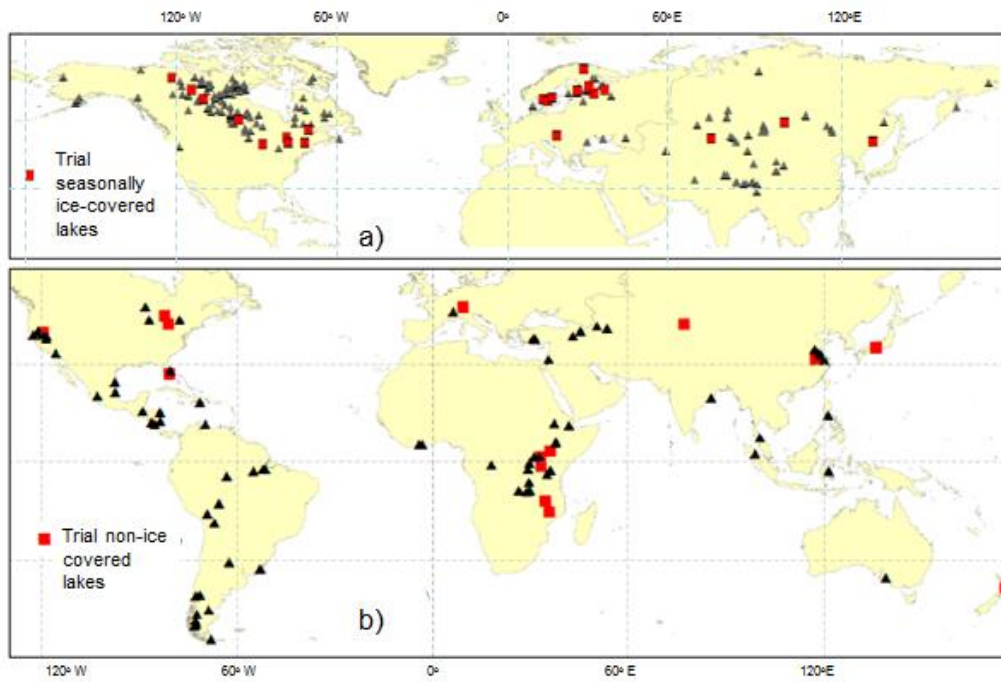


Figure 6 Location of lakes, with red square showing the trial lakes a) 160 seasonally ice-covered lakes, including 21 trial lakes and b) 86 non-ice covered lakes including 14 trial lakes

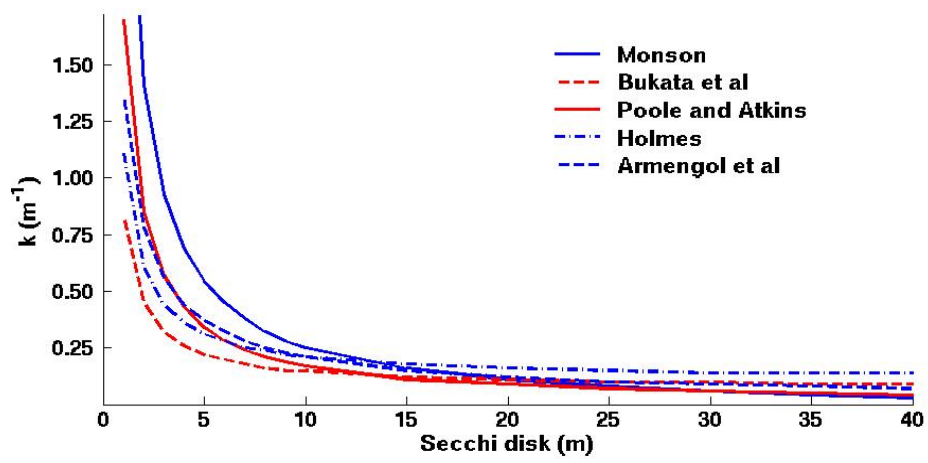


Figure 7 A comparison of 5 methods relating light extinction coefficients to Secchi disk depths, showing that all method compare reasonably well at Secchi disk depths > 10 m

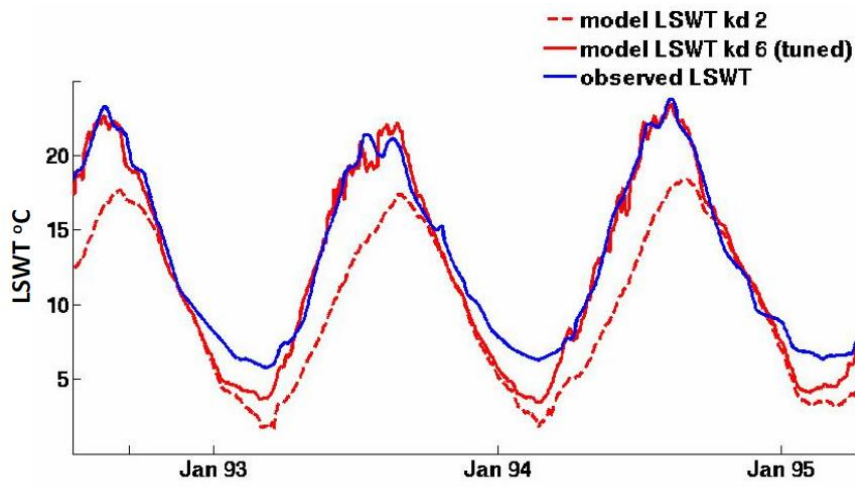


Figure 8 Lake surface water temperatures (LSWTs) for Lake Geneva, Europe (46° N 6° E), modelled with two different κ_d values (κ_{d2} κ_{d6} ; table 2) shows the substantially stronger effect of κ_d on the maximum LSWT than the minimum LSWT.

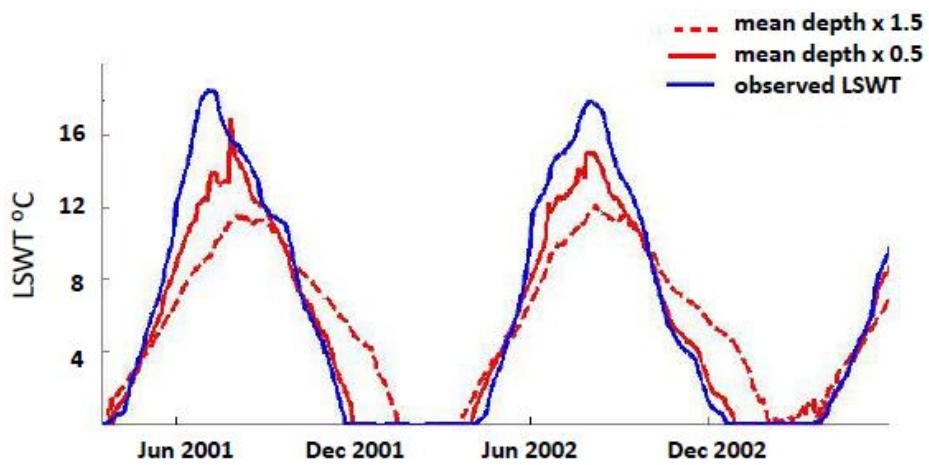


Figure 9 Effect of depth on the lake surface water temperature (LSWT) for Lake Ladoga, Russia (61° N 31° E), (mean depth 52 m), showing that when modelled with a greater depth, the lake cools later and the maximum LSWT is lower

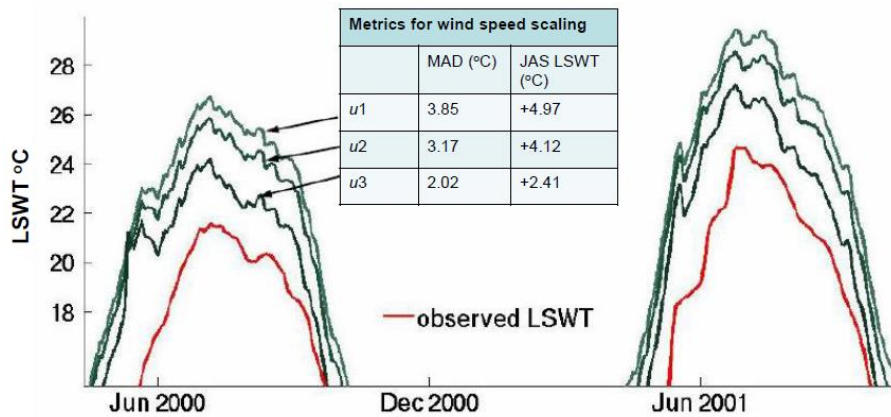


Figure 10 Effect of wind speed scalings on the modelled lake surface water temperature (LSWT) for Lake Simcoe, Canada, 44° N 79° W (depth 25 m), showing that the greatest wind speed scaling, $u3$ ($U_{\text{water}} = 1.62 \text{ m/s} + 1.17U_{\text{land}}$), in place of the unscaled wind speed, $u1$, reduces the daily mean absolute difference and July, August September LSWT mean difference by $\sim 50\%$. Modelled with untuned LSWT properties: mean lake depth (Z_{dl}), default snow and ice albedo (αI) and light extinction coefficient derived from Secchi disk depth data (κ_{sd})

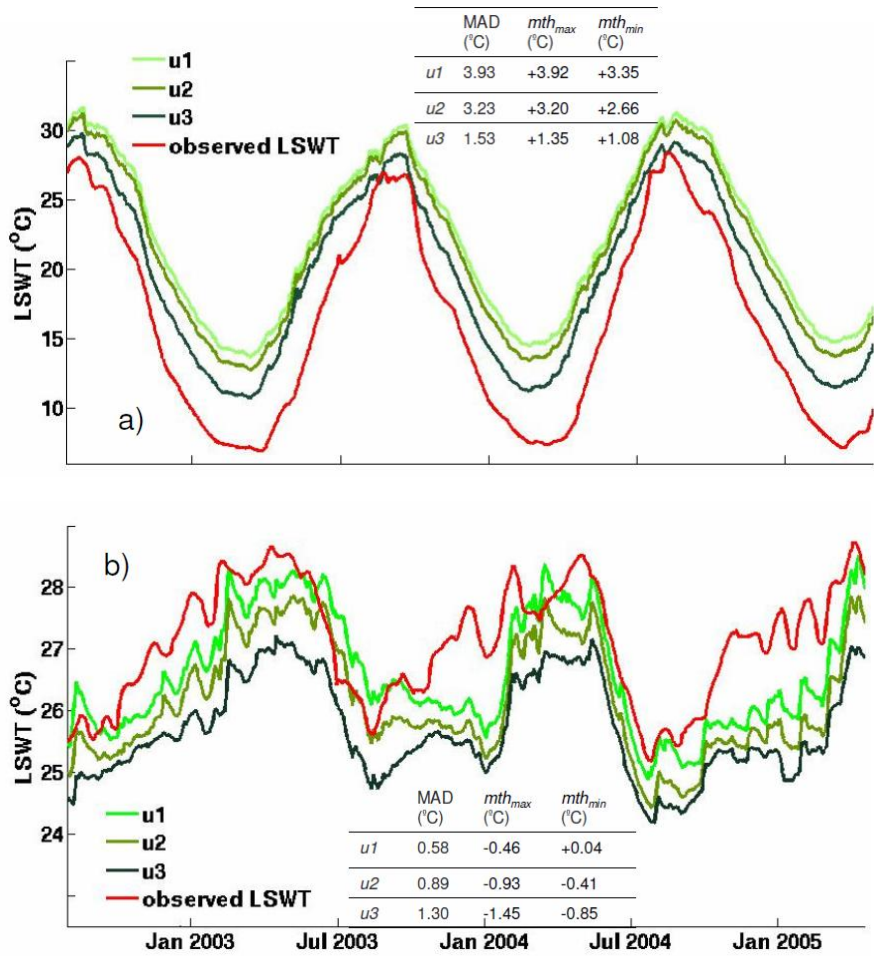


Figure 11 Effect of wind speed scaling on lake surface water temperatures (LSWT) for a temperate non-ice covered lake a) Lake Biwa, Japan (36° N 136° E) and for a tropical non-ice covered lake b) Lake Turkana, Africa (4° N 36° E) showing that the modelled LSWT for the temperate lake is better represented using $u3$ ($U_{water} = 1.62 \text{ m/s} + 1.17U_{land}$), and the modelled LSWT for the tropical lake is better represented using $u1$ (unscaled wind speed). mth_{min} (and mth_{max}) is the difference between the observed and modelled LSWTs for the month where the minimum (and maximum) LSWTs is observed

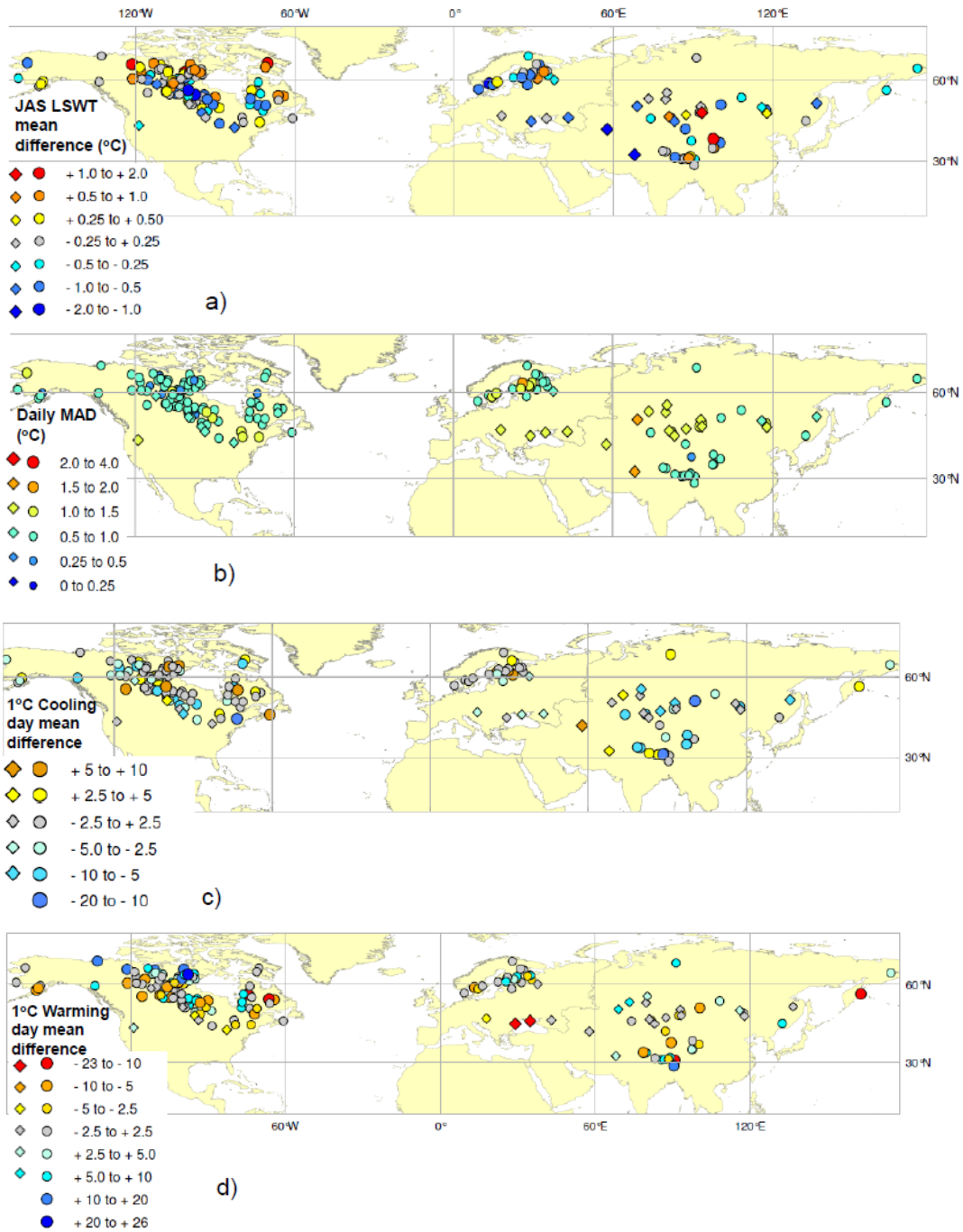


Figure 12 Tuning metric mean differences between modelled and observed LSWTs for all 160 lakes with seasonal ice-cover. The results for the 25 lakes tuned with modified tuning approach are marked by diamond symbols a) July August September (JAS) LSWT mean difference, b) daily mean absolute difference (MAD), c) 1 °C cooling day mean difference and d) 1 °C warming day mean difference

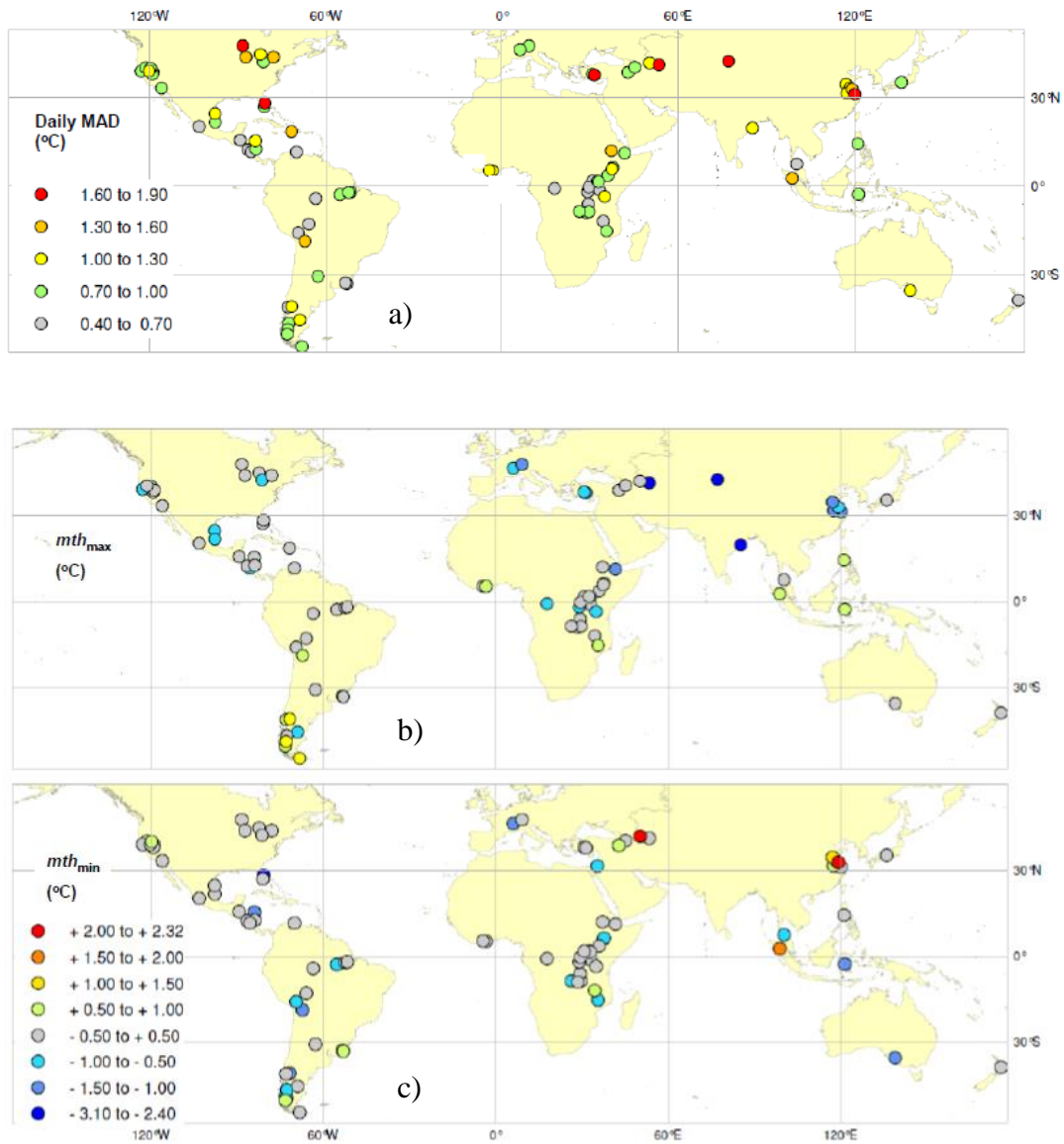


Figure 13 Tuning metric results for the 84 non-ice covered lakes a) daily mean absolute difference (MAD) between observed and modelled LSWTs, b) mth_{max} and c) mth_{min} . mth_{min} (and mth_{max}) is the difference between the observed and modelled LSWTs for the month where the minimum (and maximum) LSWT is observed

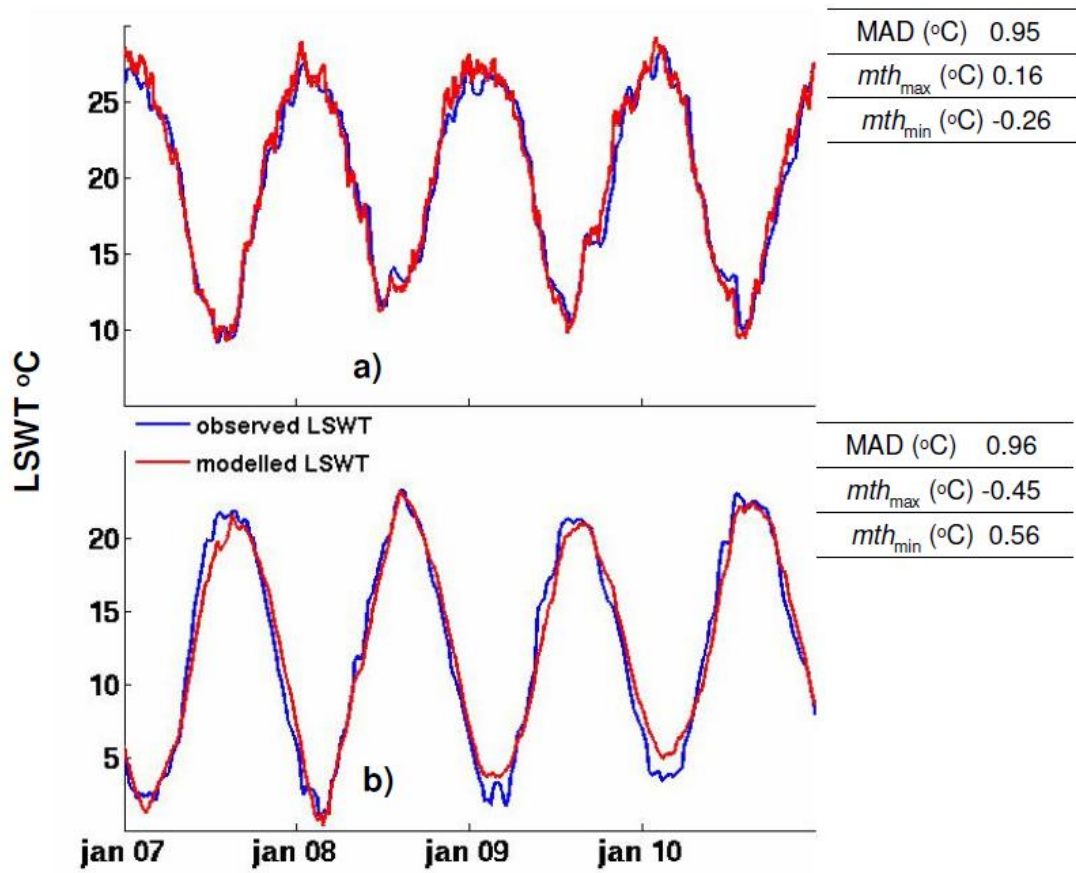


Figure 14 Observed LSWT versus tuned model LSWT for saline and high altitude lakes a) Lake Chiquita, Argentina (31° S 63° W, salinity 145 g L^{-1}) b) Lake Van, Turkey (39° N 43° E, 1638 m a.s.l., salinity 22 g L^{-1}).

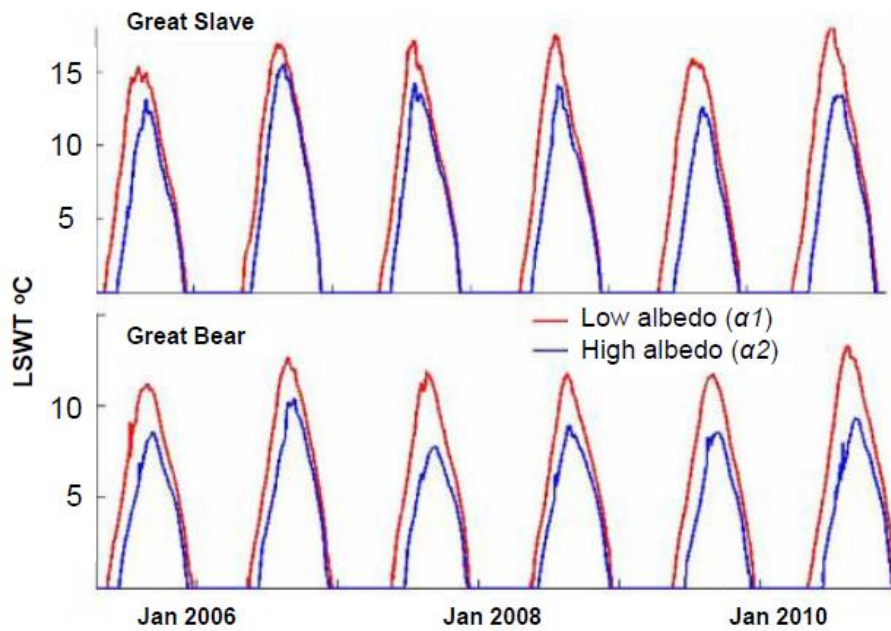


Figure 16 Lake surface water temperatures (LSWTs) for Great Bear (66° N 121° W) and Great Slave (62° N 114° W) modelled with low snow and ice albedo (default albedo, $\alpha1$: snow and white ice = 0.60 and melting snow and blue ice = 0.10) and high albedo ($\alpha2$: snow and white ice = 0.80 and melting snow and blue ice = 0.60) demonstrating that the higher snow and ice albedo delays the 1° C warming day, causing a lower July August September LSWT

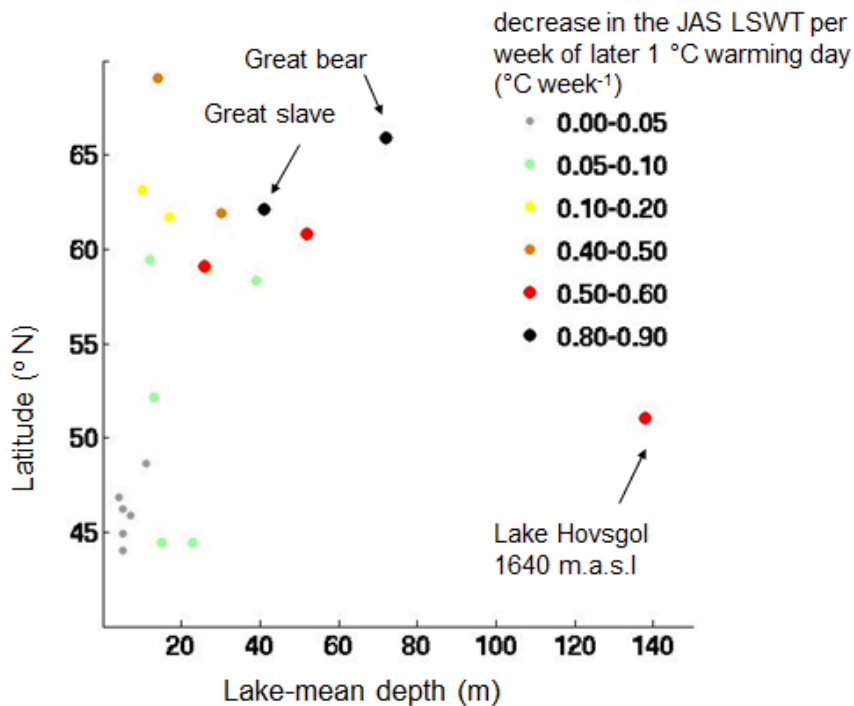


Figure 17 The relationship between latitude and lake-mean depth of the 21 trial seasonally ice-covered lakes and the decrease in the July August September (JAS) lake surface water temperature (LSWT) caused by the later 1 °C warming day (as a result of using a high albedo, α_2 : snow and white ice = 0.80 and melting snow and blue ice = 0.60 in place of the default albedo α_1 : snow and white ice = 0.60 and melting snow and blue ice = 0.10). The changes in the JAS LSWT, presented as the decrease in the JAS LSWT, per week of later 1 °C warming day, °C week⁻¹, are categorised by coloured circles. This figure indicates that high latitude and deep lakes show a larger decrease in the JAS LSWT per week of later 1 °C warming day, signifying that the LSWTs of these lakes are more responsive to changes in the 1 °C warming day, than low latitude and shallow lakes.

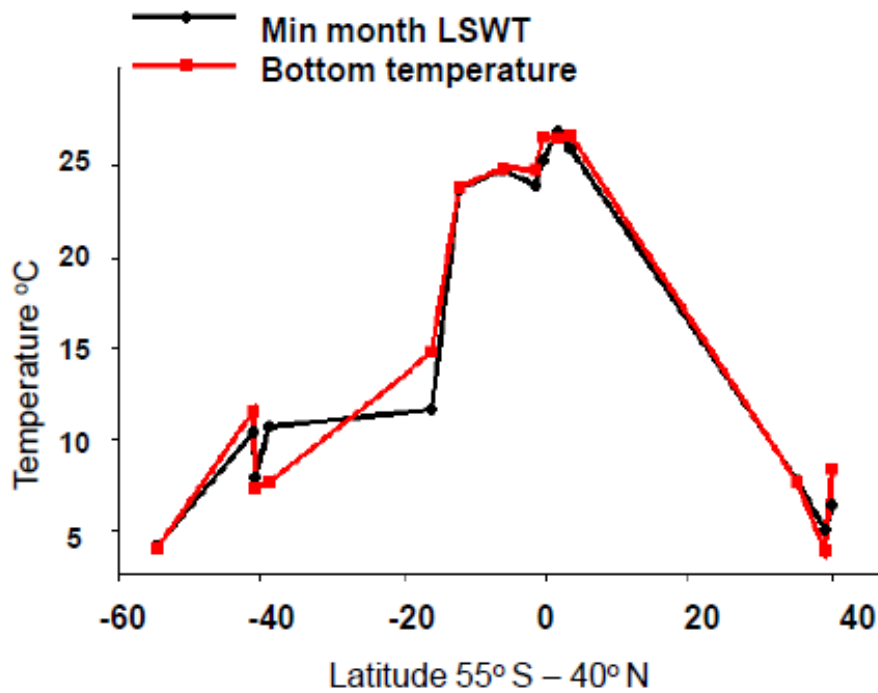


Figure 18 Comparison of lake-bottom temperatures during the stratification period, obtained from *FLake* model run using perpetual hydrological year, 2005/06 (Kirillin et al., 2011) and the monthly minimum climatology lake surface water temperature (LSWT) observations from ARC-Lake, for 14 deep (> 25 m) non-ice covered lakes (55 °S to 40 °N). The monthly minimum observed LSWTs have a ~1:1 relationship with the lake-bottom temperatures during the stratification period.

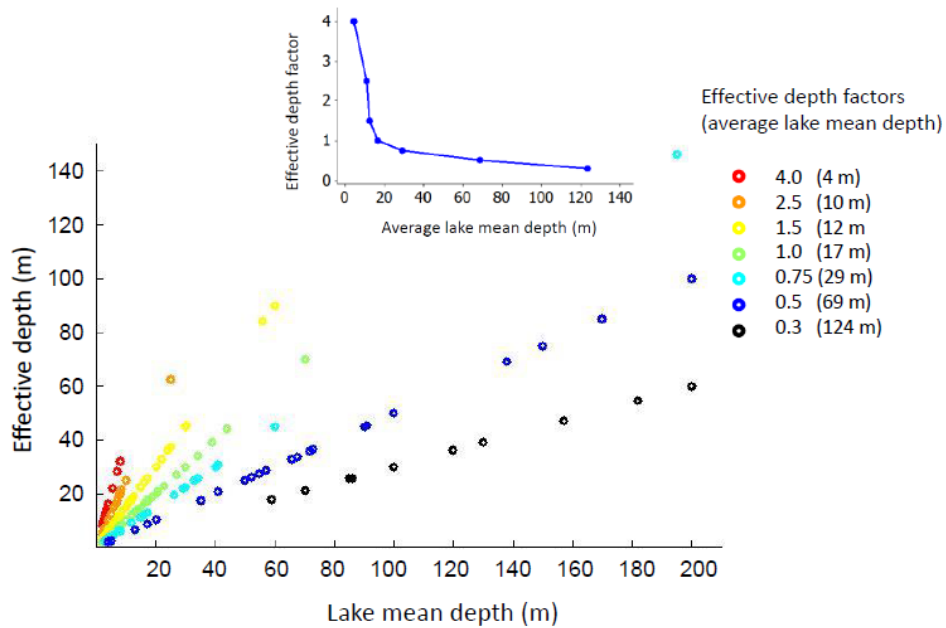


Figure 19 The lake mean depth vs. the modelled effective depth for 244 tuned lakes. Colour coding illustrates the effective depth factors. The average lake depth for each effective depth factor used in the tuning process is also given (insert). This figure demonstrates that deeper lakes are tuned to a shallower effective depth and shallower lakes to a deeper effective depth.